REVIEW ARTICLE

Greenland ice sheet mass balance: a review

IOP Publishing Reports on Progress in Physics
Rep. Prog. Phys. **78** (2015) 046801 (26pp) doi:10.1088/0034-4885/78/4/046801

Review Article

Greenland ice sheet mass balance: a review

Shfaqat A Khan[1], Andy Aschwanden[2,3], Anders A Bjørk[4], John Wahr[5], Kristian K Kjeldsen[4] and Kurt H Kjær[4]

[1] DTU Space—National Space Institute, Technical University of Denmark, Department of Geodesy, Kgs. Lyngby, Denmark
[2] Arctic Region Supercomputing Center, University of Alaska, Fairbanks, AK 99775, USA
[3] Geophysical Institute, University of Alaska, Fairbanks, AK 99775, USA
[4] Centre for GeoGenetics, Natural History Museum of Denmark, University of Copenhagen, Copenhagen, Denmark
[5] Department of Physics and Cooperative Institute for Research in Environmental Sciences, University of Colorado, Boulder, CO 80309-0216, USA

E-mail: abbas@space.dtu.dk

Received 21 July 2014, revised 14 November 2014
Accepted for publication 13 January 2015
Published 26 March 2015

Invited by Mike Bevis

Abstract

Over the past quarter of a century the Arctic has warmed more than any other region on Earth, causing a profound impact on the Greenland ice sheet (GrIS) and its contribution to the rise in global sea level. The loss of ice can be partitioned into processes related to surface mass balance and to ice discharge, which are forced by internal or external (atmospheric/oceanic/basal) fluctuations. Regardless of the measurement method, observations over the last two decades show an increase in ice loss rate, associated with speeding up of glaciers and enhanced melting. However, both ice discharge and melt-induced mass losses exhibit rapid short-term fluctuations that, when extrapolated into the future, could yield erroneous long-term trends. In this paper we review the GrIS mass loss over more than a century by combining satellite altimetry, airborne altimetry, interferometry, aerial photographs and gravimetry data sets together with modelling studies. We revisit the mass loss of different sectors and show that they manifest quite different sensitivities to atmospheric and oceanic forcing. In addition, we discuss recent progress in constructing coupled ice-ocean-atmosphere models required to project realistic future sea-level changes.

Keywords: remote sensing, glaciers, mass balance, ice-sheet modelling, Greenland ice sheet, climate change, sea-level changes

(Some figures may appear in colour only in the online journal)

1. Introduction

Ice loss from the GrIS during recent years has accelerated much faster over the last two decades (Vaughan *et al* 2013) than current models can capture (Levermann *et al* 2011, Rignot *et al* 2011). This makes the GrIS one of the largest single contributors to sea level rise over the last decade, accounting for 0.5 out of a total of 3.2 mm yr^{-1} (Cazenave and Remy 2011, Anderson *et al* 2015, Barletta *et al* 2013, Groh *et al* 2014, Shepherd *et al* 2012, Jacob *et al* 2012, Helm *et al* 2014, Khan *et al* 2014a). If this acceleration continues, the GrIS alone could contribute as much as 9 cm of sea level rise by 2050, compared to the total sea level rise of 15–20 cm observed during the last century (Church and White 2006). Therefore, the future behavior of the GrIS is of great concern, and is also one of the largest unknowns in climate research.

GrIS mass changes are due to fluctuations in surface mass balance (SMB) processes and in ice discharge at the

grounding line, both of which are dependent on atmospheric and oceanic conditions (Holland *et al* 2008, van den Broeke *et al* 2009). SMB is the difference between accumulation from precipitation (snow and rain), and mass loss from ablation (sublimation, drifting snow erosion and runoff). Dynamically-induced ice loss at the grounding line is related to accelerated flow at the marine-terminating outlets, caused by decreased buttressing and reduced basal drag that results in thinning (decreasing ice surface elevations) (Howat and Eddy 2011, Price *et al* 2011, Nick *et al* 2013). Understanding the characteristics of ice discharge and SMB prior to the last two decades (for example over the last century or millennium), combined with improved capabilities of modelling the observed short and long-term changes in Greenland's outlet glaciers, would facilitate improved predictions of future mass loss. Here we review the current state of knowledge, obtained from a variety of geodetic methods, of the GrIS mass-change over multiple timescales and its sensitivity to external forcing. We also highlight recent advances in ice-sheet modelling and what challenges need to be solved to improve ice-sheet models in future predictions.

2. Methods

Geodetic methods used to determine ice sheet volume or mass changes include airborne and satellite radar and laser altimetry (surface elevation change method), observations of ice flow of outlet glaciers using satellite interferometric synthetic-aperture radar (InSAR) (which, when combined with SMB model output, is referred to as the Input–Output method), and measurements by the Gravity Recovery and Climate Experiment (GRACE) satellite mission of changes in the gravity field caused by changes in ice sheet mass (gravimetry method). All of these methods have characteristic advantages and disadvantages. For example, airborne and satellite radar and laser altimetry have better spatial resolution than the GRACE observations, but they lack the high temporal resolution provided by the latter. Airborne and satellite radar and laser require assumptions about the firn density to convert volume to mass. In addition, satellite radar altimetry does not provide reliable results in regions of large slopes, such as those along much of the GrIS margins, and is affected by radar penetration into the snow. The Input–Output method provides the best understanding of the underlying cause of mass change in a region, but it requires knowledge of such things as outlet glacier depths, and only measures velocity along the line of site, which is problematic in many areas. Furthermore, since the net mass variations obtained using the Input–Output method are the differences between two large and, in most cases, nearly equal numbers (i.e. an SMB estimate, and an InSAR-based discharge estimate), relatively small errors in either of those numbers can lead to a relatively large error in the net mass balance. The gravimetry method provides direct estimates of mass, but has limited resolution (>250 km) and is affected by mass changes not just from ice and snow variations, but also from hydrologic and ocean mass changes, and from mass variations in the underlying solid Earth, (especially, glacial isostatic adjustment, GIA). In the remainder of this section, we provide more detailed descriptions of these methods. On local scales, other geodetic-based methods have been used to determine mass balance; for example, ground based interferometry, time lapse photography, and GPS displacement measurements of ice and bedrock. These local methods are not discussed in this paper.

2.1. Gravimetry

The GRACE mission allows for direct estimates of ice-sheet-wide mass variability, through determining the effects of that mass on the Earth's gravity field. Since its launch in March 2002, GRACE has been measuring changes in the range between two satellites that are in identical near-polar orbits (the injection altitude was 500 km), about 220 km apart. The changes in range are used to construct monthly solutions for the gravity field at the Earth's surface. Solutions are generated, for example, at the Center for Space Research (CSR) at the University of Texas (Tapley *et al* 2004), the Jet Propulsion Laboratory (JPL) at the California Institute of Technology (Landerer *et al* 2012) and the Deutsches GeoForschungsZentrum (GFZ) at Helmholtz Centre Postdam (Kusche *et al* 2009). The gravity fields consist of spherical harmonic (Stokes) coefficients, C_{lm} and S_{lm}, where l and m denote the degree and order of the harmonic coefficients, respectively; though most users replace the GRACE C_{20} coefficients with C_{20} estimates inferred from satellite laser ranging (Cheng and Tapley 2004).

The GRACE gravity solutions allow users to determine monthly mass fluctuations averaged over scales of a few hundred km and greater. Mass variability from individual glaciers, though, cannot be resolved. The contributions from all glaciers within a region are automatically included in a regional estimate, but it is not possible to determine how much each glacier contributed (Velicogna *et al* 2014). Unlike other methods, GRACE provides a direct estimate of mass balance, without requiring any intermediate assumptions (other than Newton's Law of Gravity). However, the GRACE gravity fields represent the total gravity variability from all geophysical sources, and cannot distinguish between contributions from ice sheet mass, and those from such things as mass variations within the atmosphere, ocean, and liquid water storage on land; or from signals associated with mass variability in the solid Earth: e.g. episodic (earthquake) processes, and glacial isostatic adjustment (the viscoelastic response of the solid Earth to glacial unloading over the last several thousand years) (Sutterley *et al* 2014). For Greenland, none of these other sources of gravity is likely to be a serious problem. The GRACE centers use model output to remove atmospheric and oceanic signals before constructing the monthly gravity fields. Greenland is far enough from other land areas that the effects of liquid land water storage do not cause appreciable contamination of the Greenland results. And, Greenland and the surrounding region do not experience earthquakes that are large enough to significantly affect the Greenland mass estimates. The GIA signal is potentially more of an issue. Since it is linear and cannot be separated from a linear trend in present-day ice mass, it should be independently modelled and removed. However, existing

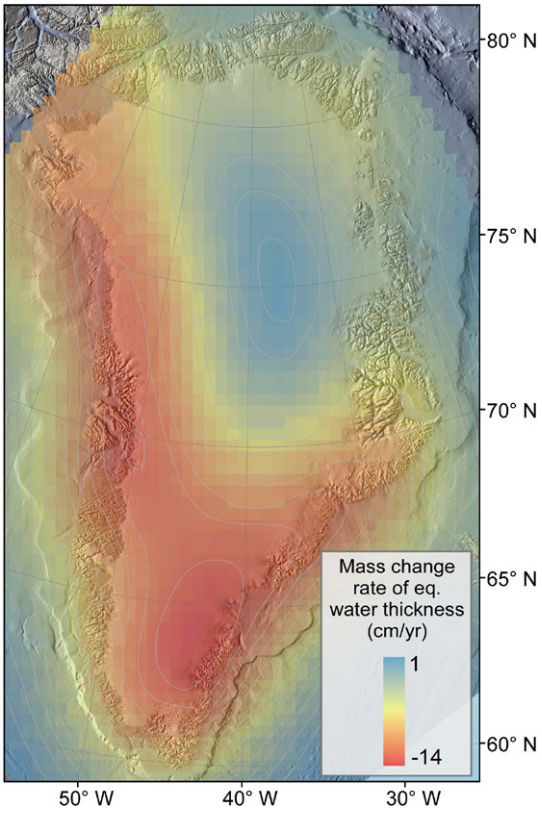

Figure 1. Average April 2002–June 2014 mass change rate of the Greenland ice sheet extracted from GRACE, in units of centimetres per year of equivalent water thickness.

GIA models suggest that this correction is rather small for Greenland, about $-7 \pm 19\,\mathrm{Gt\,yr^{-1}}$ (Velicogna and Wahr 2006).

Figure 1 shows the average rate of mass change across the GrIS between April, 2002 and July, 2014, determined from the CSR GRACE fields. The GRACE C_{20} gravity coefficients are replaced with those estimated from satellite laser ranging (Cheng and Tapley 2004). Degree-one coefficients are also included, computed as described by Swenson *et al* (2008). The method described in Wahr *et al* (1998) is used to transform the gravity coefficients into surface mass coefficients. Those coefficients are used to compute surface mass on a 0.5 × 0.5 degree grid, smoothed with a Gaussian smoothing function with a 250 km half-width. Figure 2 shows the time series of the total mass change for the GrIS, estimated from GRACE monthly mass solutions for the period from April, 2002 to June, 2014.

2.2. Surface elevation changes

Airborne or satellite-borne radar or laser sensors are used to repeatedly map glacier surface elevations to estimate volume changes. The technique can provide a detailed pattern of mass imbalance for major drainages and glaciers.

2.2.1. Satellite laser altimetry. Satellite laser altimetry from the Geoscience Laser Altimeter System (GLAS) instrument on the Ice, Cloud, and land Elevation Satellite (ICESat) provided global measurements of surface elevation from 2003 to 2009, and repeated those measurements along almost identical tracks (separated by a few hundred meters), typically 2–3 times a year. The primary goal of the mission was to measure changes in ice volume over time.

The latest ICESat Release 34 data (Zwally *et al* 2014) are available from the National Snow and Ice Data Center (https://nsidc.org/data/icesat/). The level-2 altimetry product (GLA12) provides surface elevations for ice sheets and consists of 18 campaigns. The satellite laser footprint diameter is 30–70 m and the distance between footprint centres is approximately 170 m. The dominant biases come from pointing errors and saturation errors. For ICESat elevations that have been corrected for both pointing and saturation errors, and that have been filtered for surface roughness and atmospheric scattering and corrected for intercampaign elevation biases (Hofton *et al* 2013, Borsa *et al* 2014), the single-shot accuracy is $\sigma_{\mathrm{ICESat}} = 0.1$ m. Figure 3 shows elevation change rates during 2003–2009 derived from ICESat.

2.2.2. Airborne laser altimetry

Land, vegetation, and ice sensor (LVIS). NASA's Land, Vegetation, and Ice Sensor (LVIS) is a scanning laser altimeter instrument that provides data on surface topography and vegetation coverage. LVIS has a scan angle of about 12 degrees, and can cover about 2 km swaths of surface from an altitude of 10 km. LVIS flew aboard the DC-8 and P-3B airborne laboratories until 2011, and since then in a King Air B-200, a Gulfstream G-V and an HU-25C Guardian Falcon. LVIS data were collected as part of NASA funded campaigns and are available from 2009 to 2013 through the National Snow and Ice Data Center (http://nsidc.org/data/ilvis2). Data from a single pre-IceBridge campaign in 2007 are available from http://nsidc.org/data/blvis0. Figure 4 shows the surface elevation over the frontal portion of Jakoshavn Isbræ in west Greenland. The high pixel resolution of LVIS allows detection of small icebergs in the Kangia Fjord. LVIS can be used to validate and calibrate measurements by, for example, ICESat (Hofton *et al* 2008) and CryoSat-2 elevations.

Airborne topographic mapper (ATM). The ATM, developed at NASA's Wallops Flight Facility (WFF) in Virginia, is a scanning laser altimeter that measures ice surface elevation from an aircraft at an altitude of between 400 and 800 m above ground level. NASA has flown ATM surveys in Greenland nearly every year since 1993 aboard the NASA DC-8, twin-otters (DHC-6), C-130's, and other P-3 aircraft. The ATM has been participating in NASA's Operation IceBridge since 2009. The NASA IceBridge and pre-IceBridge ATM Level-2 Icessn Elevation, Slope, and Roughness (BLATM2) data from 1993 to 2013 are available through the National Snow and Ice Data Center (http://nsidc.org/data/ilatm2).

ATM flights are mainly concentrated along the main flowlines of outlet glaciers. In particular, the frontal portion of Jakobshavn Isbræ has been very well surveyed over the last two decades. The ATM measurements have an elevation accuracy of $\sigma_{\mathrm{ATM}} = 0.1$ m (Krabill *et al* 2002).

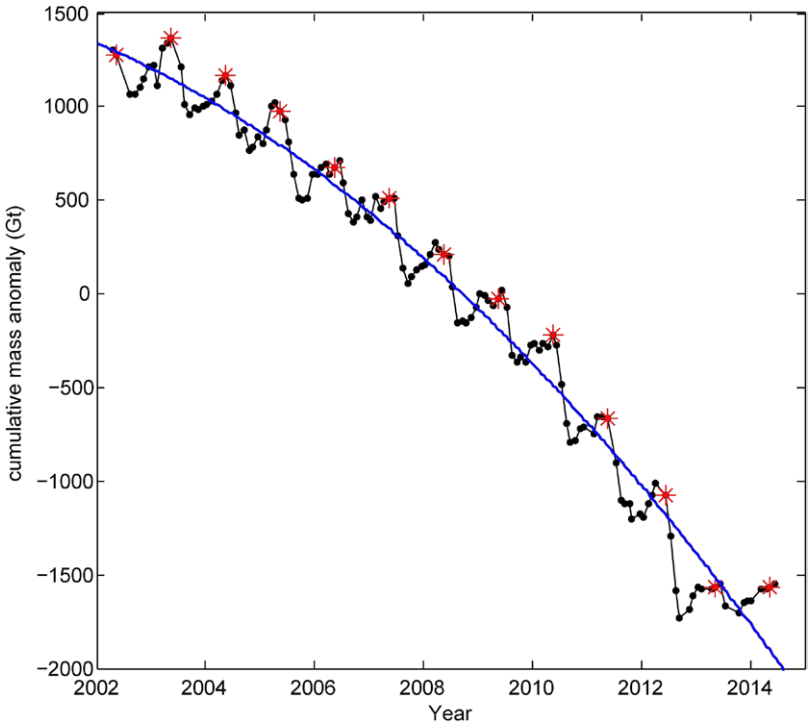

Figure 2. Time series of the cumulative ice sheet-wide mass anomaly of the GrIS extracted from GRACE, in gigatonnes. The red asterisks denote June values (or May values, for years when June is missing), and best-fitting trend quadratic trend (blue).

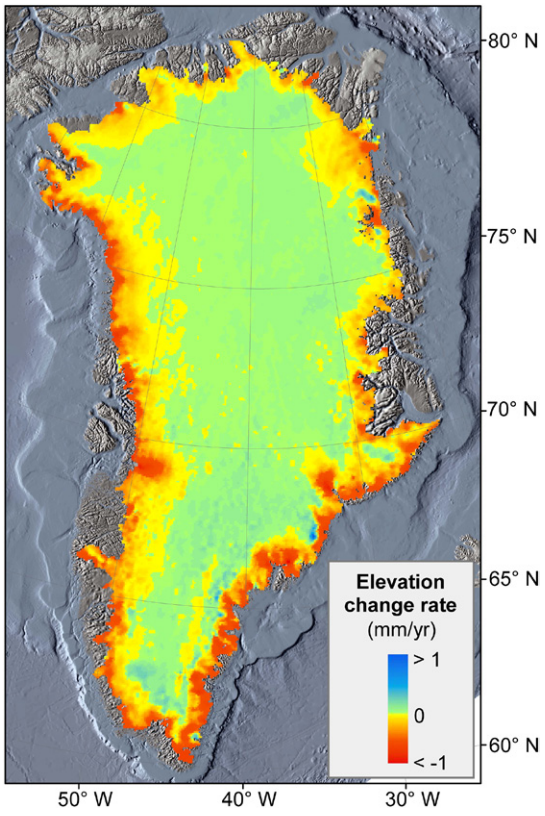

Figure 3. Elevation change rates during 2003–2009, as derived from ICESat.

Merging ICESat, ATM, and LVIS. Ice loss from the GrIS is dominated by loss in the marginal areas. Dynamically-induced ice loss and the associated ice surface lowering is often largest close to the glacier calving front and may vary from rates of tens of meters per year to a few meters per year over relatively short distances (5–10 km) (Howat *et al* 2007, Stearns and Hamilton 2007, Liu *et al* 2012). Hence, high spatial resolution data are required to accurately estimate volume changes. To improve volume change estimates, especially those caused by marginal thinning, ICESat data may be supplemented with, for example, altimeter surveys from ATM and LVIS (Kjeldsen *et al* 2013, Schenk *et al* 2014). A recent study by Kjeldsen *et al* (2013), shows a difference of about 11% between ice loss estimates obtained using ICESat data solely, and using ICESat data supplemented with airborne laser data from ATM and LVIS. Other studies, for instance Howat *et al* (2008), supplement ICESat derived surface elevation changes with differenced Advanced Spaceborne Thermal Emission and Reflection (ASTER) radiometer digital elevation models of outlet glaciers in southeastern Greenland, to obtain improved regional volume-loss rates.

2.2.3. Satellite radar altimetry. Radar altimetry provides ice-sheet volume changes from surface elevation changes. Among all geodetic techniques satellite radar altimetry provides the longest continuous record of ice-sheet-wide volume changes. The European Space Agency's (ESA) European Remote Sensing 1 and 2 (ERS-1 and ERS-2) satellite radar altimeters and the Environmental Satellite (Envisat) radar provide ice-sheet-wide observations of surface changes from May 1992 to September 2010. The Envisat altimeter, launched in April 2002 followed the same 35 d orbit as ERS-1 and ERS-2 to ensure a homogeneous time series over more than two decades (Remy and Parouty 2009, Khvorostovsky 2012).

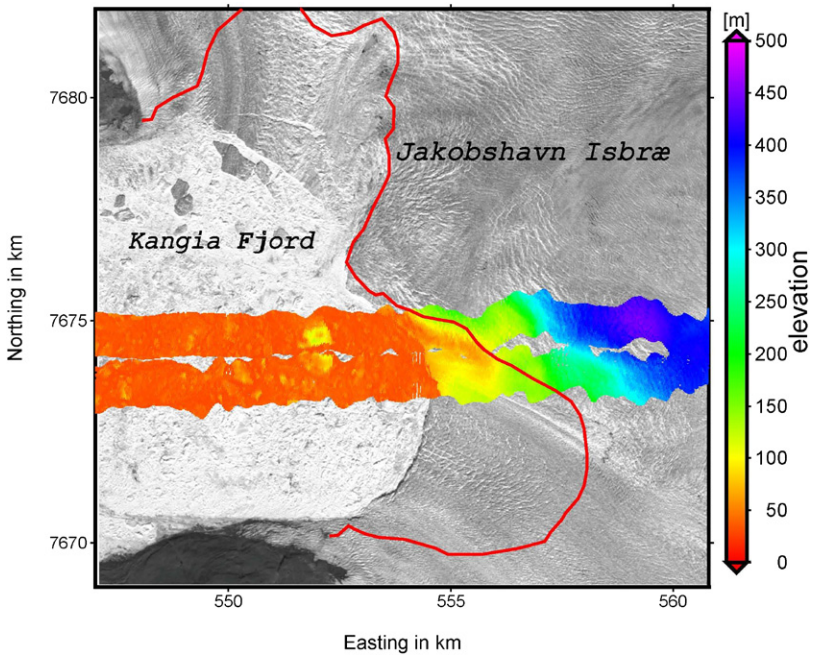

Figure 4. Surface elevation over the Jakobshavn Isbræ measured by LVIS in 2007. The background shows SPOT imagery from August 2007. The red curve represents the calving front in August 2013.

To obtain surface elevations, corrections are applied for the lag of the leading-edge tracker, surface scattering, dry atmospheric mass, water vapour, ionosphere, slope-induced error, solid Earth tide, and ocean loading tide (Wingham *et al* 1998, Davis and Ferguson 2004, Remy and Parouty 2009, Khvorostovsky 2012). Biases between waveform parameters are estimated to create their time series along with time series of surface elevation change for determining correction, which account for the correlation between backscattered power and surface elevation change (Davis and Ferguson 2004, Wingham *et al* 2008, Remy and Parouty 2009, Khvorostovsky 2012). Radar altimetry suffers from problems with surface slope; therefore, great caution should be made when using data over coastal regions with rough terrain. Furthermore, the scale of outlet glaciers in Greenland (5–10 km wide) is small in comparison to the size of the pulse-limited altimeter footprint (nominally 2–10 km in diameter), which leads to significantly reduced data volumes in the ice marginal regions. Additionally, when merging ERS-1, ERS-2 and Envisat data, inter-satellite biases have to be estimated and removed (Khvorostovsky 2012).

2.2.4. Ice volume to mass. The conversion of a volume loss rate obtained from any of the above altimetric techniques, into a mass loss rate, requires assumptions about density. To estimate elevation changes due to firn compaction, recent studies have used a simple firn model (Li and Zwally 2011, Zwally *et al* 2011, Khan *et al* 2014a) that includes melt and refreezing (Reeh 2008). The firn model is forced by annual temperature, accumulation, melt, and refreezing from one of several regional models, such as BOX (Box 2013, Box *et al* 2013), MAR (Fettweis *et al* 2011), RACMO2 (Ettema *et al* 2009), HIRHAM (Christensen *et al* 2006), or the model by Hanna (Hanna *et al* 2011). Figure 5 shows elevation change rates due to firn compaction as a function of time using temperature, accumulation, melt, and refreezing from the regional climate model RACMO2 (Khan *et al* 2014). The height changes due to firn compaction correspond to ice-sheet-wide volume changes of $-11.9 \pm 3.4\,\mathrm{km^3\,yr^{-1}}$ during 2003–2006, $-29.8 \pm 3.4\,\mathrm{km^3\,yr^{-1}}$ during 2006–2009, and $-41.0 \pm 3.4\,\mathrm{km^3\,yr^{-1}}$ during 2009–2012. Other studies, for example Sørensen *et al* (2011), used forcing from the HIRHAM5 regional climate model (Christensen *et al* 2006) and obtained ice-sheet-wide firn correction of $-19\,\mathrm{km^3\,yr^{-1}}$ for 2003–2008. For comparison, using the model of Khan *et al* (2014a) gives an average firn correction for 2003–2008 of $-18\,\mathrm{km^3\,yr^{-1}}$.

2.2.5. Correction for elastic uplift of the bedrock. Observed ice surface elevation changes must be corrected for bedrock movement caused by elastic uplift from present-day mass changes (Khan *et al* 2010b, Bevis *et al* 2012). To demonstrate the order of this correction and its evolution over time, we use mass loss estimates from Khan *et al* (2014a) and convolve with Green's function for vertical displacements derived by Boy (Petrov and Boy 2004) for the Preliminary Reference Earth Model (Dziewonski and Anderson 1981). Figure 6 shows predicted vertical deformation of bedrock during 2003–2006, 2006–2009, and 2009–2012, respectively. The correction due to elastic uplift converted to ice volume corresponds to $3.6 \pm 0.3\,\mathrm{km^3\,yr^{-1}}$ during 2003–2006, $8.2 \pm 0.3\,\mathrm{km^3\,yr^{-1}}$ during 2006–2009, and $9.9 \pm 0.4\,\mathrm{km^3\,yr^{-1}}$ during 2009–2012.

2.2.6. Correction for glacial isostatic adjustment. Ice surface elevation changes must be corrected for the viscous response of the lithosphere to past glacial history, or glacio-isostatic adjustment. Figure 7 shows uplift rates derived from ICE-5G (VM2 L90) model version 1.3 (Peltier 2004). Grid data files

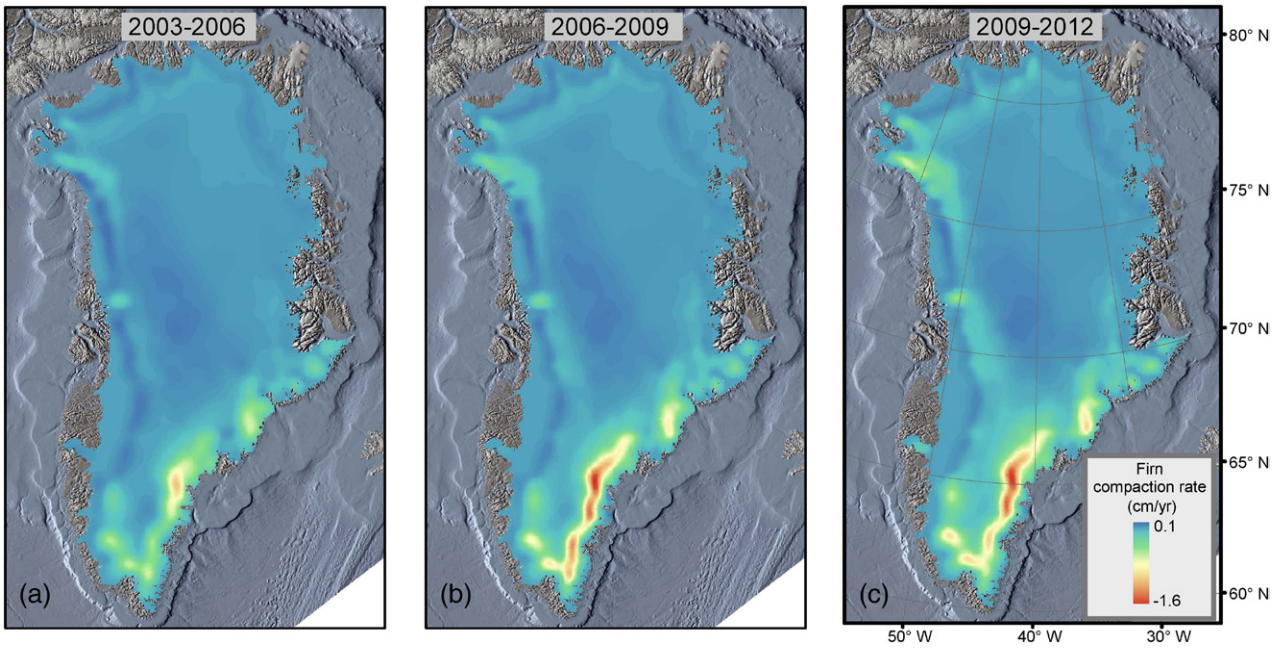

Figure 5. Elevation change rates due to firn compaction during (*a*) 2003–2006, (*b*) 2006–2009, and (*c*) 2009–2012 using climate inputs from RACMO2.

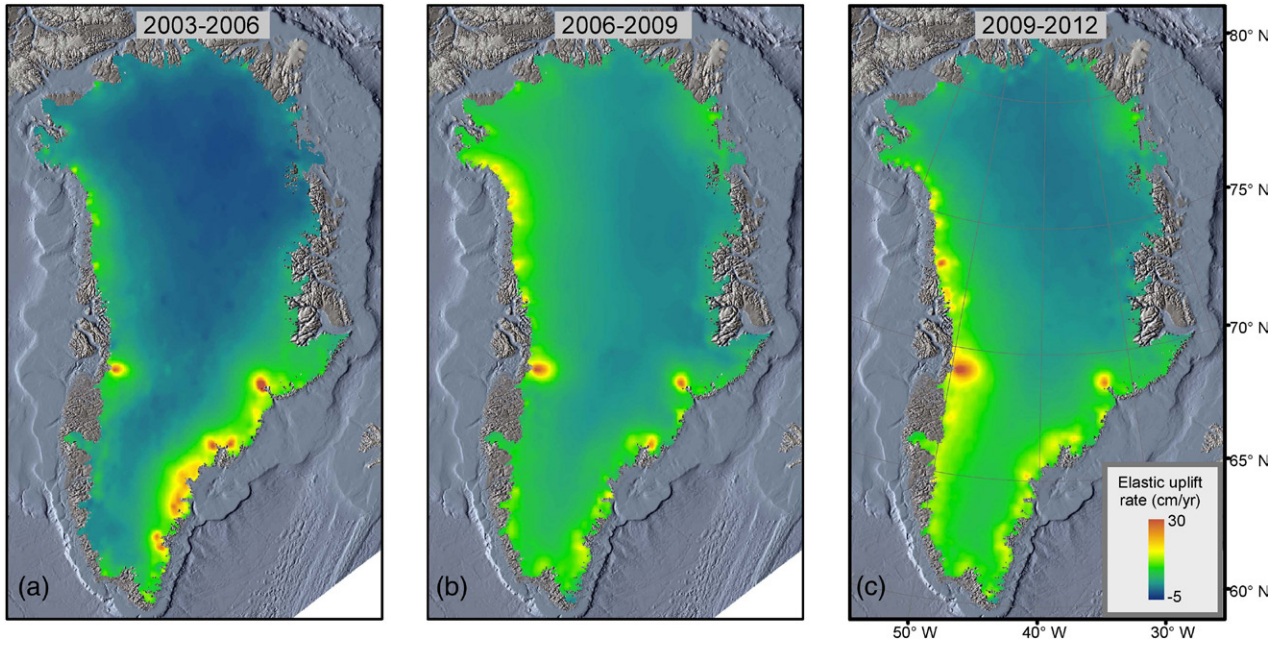

Figure 6. Predicted elastic uplift of the bedrock due to present-day ice loss during (*a*) April 2003–April 2006, (*b*) April 2006–April 2009, and (*c*) April 2009–April 2012.

are available from (www.atmosp.physics.utoronto.ca/~peltier/data.php). Rates of vertical land motions caused by GIA can be considered constant over an inter-decadal timescale. We obtain an ice-sheet-wide GIA correction, that converts to an ice volume of $-0.1\,\mathrm{km^3\,yr^{-1}}$. When considering ice-sheet-wide volume loss, the positive rates in north Greenland (uplift of about $8\,\mathrm{mm\,yr^{-1}}$) seem to largely cancel the negative values in central Greenland (subsidence of about $4\,\mathrm{mm\,yr^{-1}}$), resulting in an overall small GIA correction of $-0.1\,\mathrm{km^3\,yr^{-1}}$. However, over smaller regions, for example the northeast sector of the GrIS, the GIA correction is $0.9\,\mathrm{km^3\,yr^{-1}}$. Other GIA models, for example HUY2 (Simpson *et al* 2011), give a similar ice-sheet-wide correction of $<1\,\mathrm{km^3\,yr^{-1}}$.

2.3. The input–output method

The input–output method quantifies the difference between the SMB and ice discharge, D, at the grounding line (van den Broeke *et al* 2009).

$$\mathrm{MB} = \partial M / \partial t = \mathrm{SMB} - D$$

Consequently, the method provides estimates of SMB and discharge separately at individual glacier drainage basins

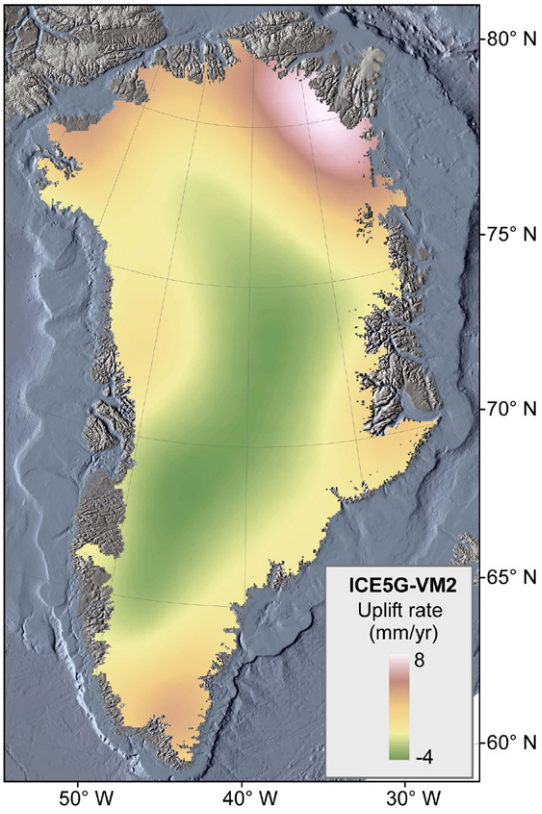

Figure 7. Predictions of GIA uplift rates in mm/yr derived using ICE-5G.

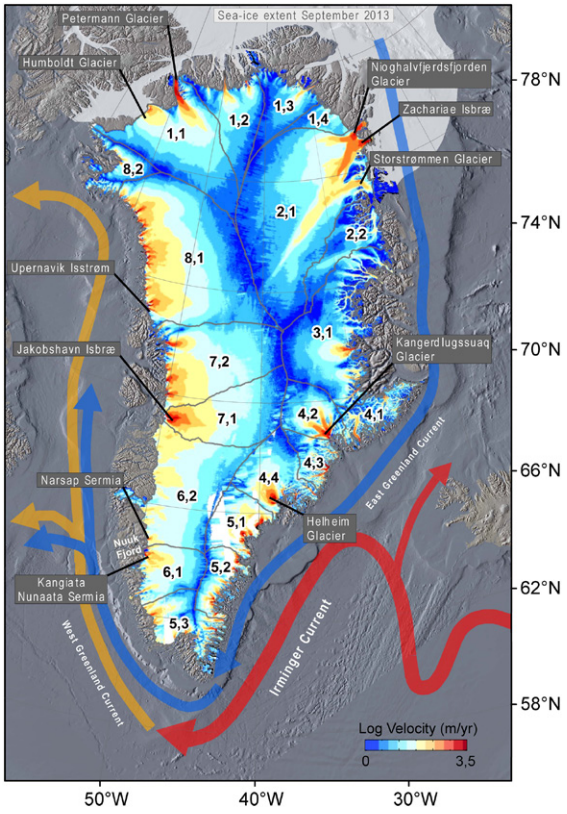

Figure 8. Map of observed surface speeds from Joughin *et al* (2010) and the major drainage basins. Arrows denote the Irminger current (red), the East Greenland current (blue arrow), and the West Greenland current (orange arrow).

(Rignot and Kanagaratnam 2006, Howat *et al* 2007, Rignot *et al* 2008, van den Broeke *et al* 2009).

SMB is constructed from regional atmospheric climate models and provides sub-daily predictions at high spatial resolution. The SMB model errors depend on the location and size of the study area. Errors are typically 5–20%. However, larger errors are likely in areas with extreme precipitation or melting (low or high). One other important issue is the general assumption of the altitude of the 'grid-cell' under consideration when downscaling numerical climate model. This can often provide major errors. Model resolutions typically range from approximately 10 to 30 km or more.

To estimate D it is necessary to measure ice velocity and ice thickness. However, often no measurement of ice thickness at the glacier grounding line is available, and so

$$D = F + \delta\mathrm{SMB}_\mathrm{g} + \delta D_\mathrm{g}$$

where δD_g is the ice storage due to glacier dynamics between the flux gate and the grounding line, and $\delta\mathrm{SMB}_\mathrm{g}$ is the SMB anomaly between the flux gate and the grounding line. The ice flux through a flux gate is,

$$F = \nu f h w \rho$$

where ν is the gate-perpendicular ice surface velocity and f is the mean ratio of surface to depth-averaged velocity, ρ is the ice density, and w and h are the width and height of the ice column.

To estimate the ice sheet mass anomaly, δM, the time-integrated (cumulative) anomalies of δSMB and δD are required (Broeke *et al* 2009),

$$\delta M = \int \mathrm{d}t\,(\delta\mathrm{SMB} - \delta D)$$
$$= \int \mathrm{d}t\,(\delta\,(\mathrm{SMB} - \mathrm{SMB}_0) - \delta\,(D - D_0)\,)$$

with SMB_0 and D_0 the reference surface mass balance and discharge.

Velocity maps are derived from, for example, InSAR data from the RADARSAT-1 satellite. Measurements are obtained from overlapping images and represent the mean velocity over days to months. The formal errors determined from radar-derived speeds compare very well with those derived from GPS data (Joughin 2002). In general, formal errors are well below the observed speeds of glacier change. However, velocity maps are also derived by applying feature tracking between pairs of optical images (for example Landsat-5 TM Band 4 and Landsat-7 ETM+ Band 8). For some outlet glaciers, e.g. Helheim Glacier, Kangerdlugssuaq Glacier, and Jakobshavn Isbræ, the velocity is mapped at a high frequency (approximately monthly) (Howat *et al* 2011, Bevan *et al* 2012), allowing sub-annual estimation of ice discharge. The largest uncertainty in ice discharge calculations comes from areas of no or very poor ice thickness observations. The recent bed map of Bamber *et al* (2013a) derived from

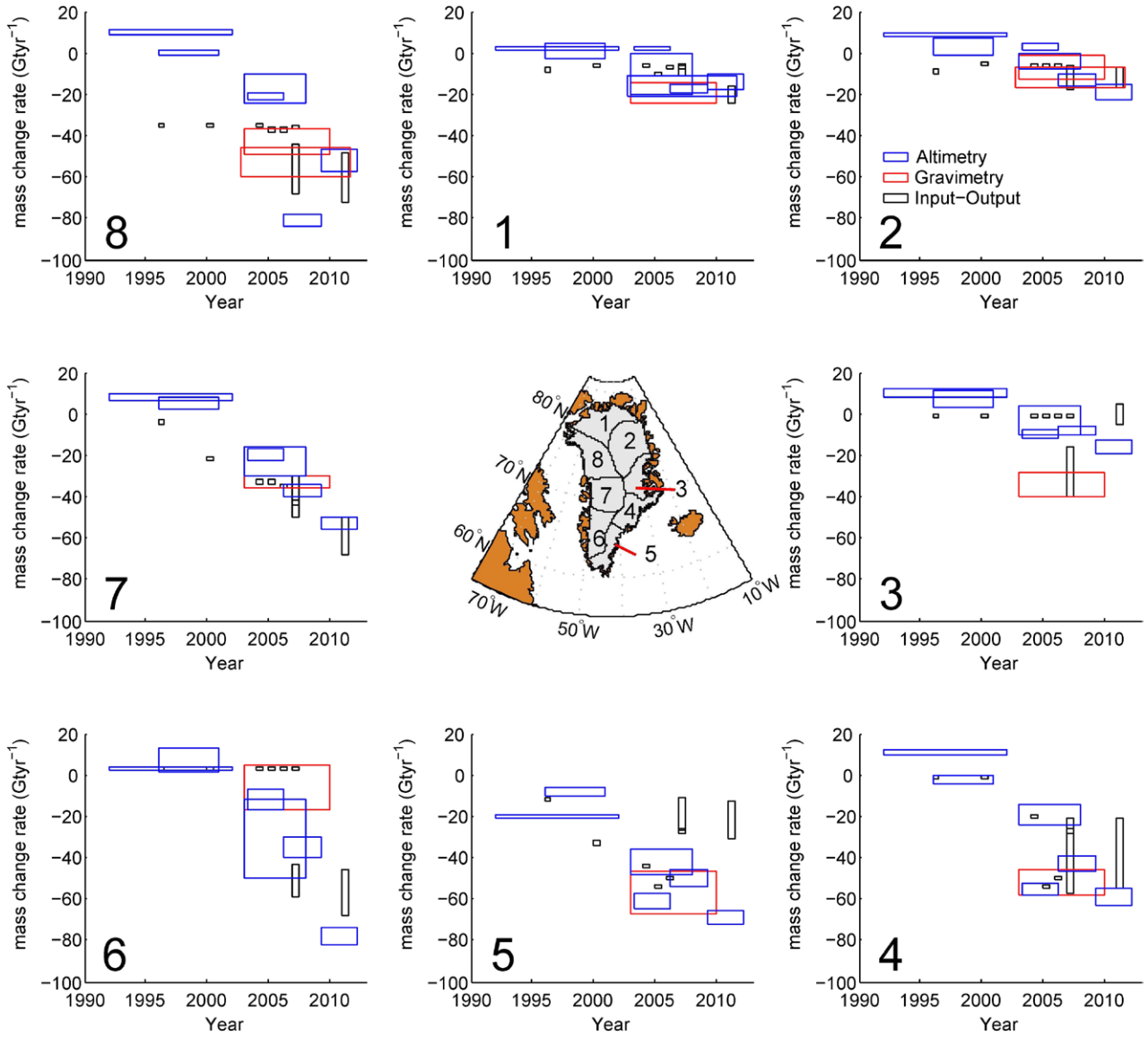

Figure 9. Mass change estimates for Greenland's major drainage basins.

a combination of multiple airborne ice thickness surveys undertaken between the 1970s and 2012 has made significant improvements. However, areas with only a few measurements are still present. Further advances in improving bed topography have recently been made by applying a mass conservation scheme which incorporates surface velocity measurements and radar measurements of the bed (Morlighem *et al* 2014). Overall, errors in bed elevation range from a minimum of ±10 m to about ±300 m Bamber *et al* (2013a). For many outlet glaciers, the thinning rate over the last decade has increased to >10 m yr^{-1}; thus, the temporal evolution of ice thickness has to be taken into account for precise ice flux estimation. Furthermore, flow speed, and therefore discharge, can vary significantly on sub-annual timescales (Howat *et al* 2007, Joughin *et al* 2008, Howat *et al* 2011). Therefore, Sub-annual velocity maps may improve mass change rates. A snapshot of a few velocity maps may under-sample the discharge signal and yield incorrect cumulative changes in mass (Howat *et al* 2011).

3. Ice mass changes over multiple timescales

3.1. Catchment-wide mass loss during last decade

To study the spatial and temporal variability of the mass change components, we divide the GrIS into a set of major drainage basins numbered from 1 to 8 (see figure 8) representing (1) north, (2) northeast, (3) east, (4) southeast, (5) south, (6) southwest, (7) west, and (8) northwest. These major basins are further divided into sub-drainage basins (see figure 8).

The ice-sheet and catchment-wide mass balance estimates have been greatly improved over the past few decades by the use of satellite geodesy measurements. Observations show a significant increase in ice loss associated with the speed up of

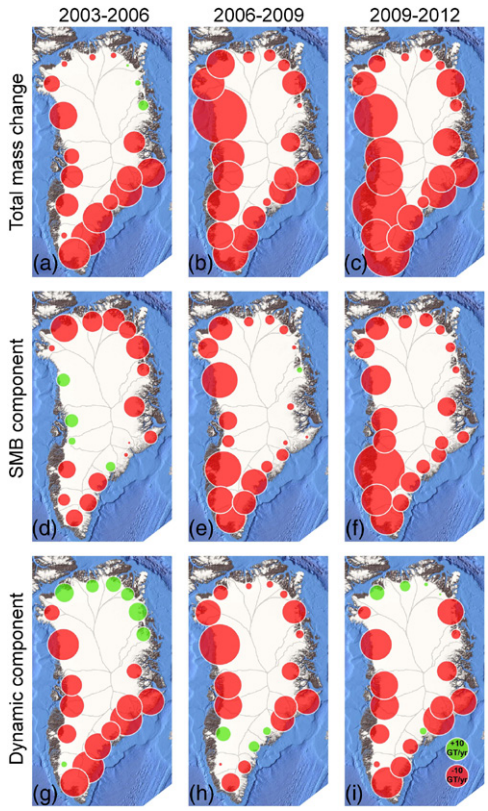

Figure 10. Rates of total ice mass change, the SMB component, and the dynamic component during 2003–2006, 2006–2009, and 2009–2012 (Khan *et al* 2014a). Red circles denote mass loss, and green circles denote mass gain.

glaciers in southeast and northwest Greenland starting in 2003 and 2005, respectively, followed by a slowdown of ice speed between 2006 and 2009. These short-term perturbations have a significant impact on the mass balance averaged over decadal scales. To illustrate the temporal and spatial variability of the GrIS over the last two decades, we consider the mass change in each major drainage basin defined in figure 8.

Southeast: since 2000, the rates of discharge from several marine-terminating glaciers along the southeast coast, notably Kangerdlugssuaq (basin 3.3), Helheim (basin 4.1), and the many glaciers in basin 4.2, have more than doubled as a result of significant accelerations in flow speed (Rignot and Kanagaratnam 2006) (see figures 9 and 10). The sudden speed-ups of those glaciers coincided with observed thinning rates of 15–90 m yr^{-1} (Joughin *et al* 2004, Howat *et al* 2005, 2008, Stearns and Hamilton 2007), which indicates a significant mass imbalance in this area of the ice sheet. Recent studies suggest increased melt-induced ice loss over the last decade, and an almost equal split between surface processes and ice discharge in this region (van den Broeke *et al* 2009, Sasgen *et al* 2012). However, in the last few years (2009–2012) the rate of discharge has decreased (Enderlin *et al* 2014).

In southwest Greenland (drainages 6.2 and 6.1), where the ice sheet margin is typically located up to 100 km inland of the coastline, there are few marine terminating glaciers and ice loss is dominated by atmospheric forcing (van den Broeke *et al* 2009, Wake *et al* 2009, Tedesco *et al* 2013). The ice sheet has a gentler slope compared to the southeast coast, and surface melting occurs much farther inland. The few glaciers terminating in long fjords do, however, also undergo dynamic thinning, but to a lesser degree than the marine terminating glaciers in the northwest and southeast. Such has been the case for the Sermilik Bræ (drainage zone 5), whose mass loss in the second half of the twentieth century was equally split between an SMB anomaly and a discharge anomaly (Podlech *et al* 2004). The large marine terminating glacier Kangiata Nunata Sermia (KNS) has also been a major contributor to dynamic-induced driven mass loss in the region (drainage basin 6.2), undergoing speed up and thinning in 2010 (Van As *et al* 2014).

Jakobshavn Isbræ (basin 7.1) in west central Greenland has long been regarded as Greenland's fastest-flowing glacier, and drains about 6% of the GrIS area (Motyka *et al* 2010). The floating ice tongue has been retreating for more than a century (Csatho *et al* 2008), resulting in increased discharge. The largest observed rapid retreat and massive ice loss began in 1998 (Motyka *et al* 2010). Recently speeds of more than 17 km yr^{-1} have been recorded, making it the fastest glacier in both Greenland and Antarctica (Joughin *et al* 2014b). The influence of warm oceanic water on the calving glacier front has been a driver for episodes of rapid retreat and speed-up (Holland *et al* 2008). It is believed that the glacier will continue to undergo episodes of rapid dynamic changes, because the front has presently reached an overdeepening, allowing further retreat (Morlighem *et al* 2013, Joughin *et al* 2014b). Model studies show that Jakobshavn Isbræ is likely to continue its high rate of mass loss into the future, with substantial contributions from both increased SMB-induced mass loss and increased ice discharge (Price *et al* 2011, Nick *et al* 2013).

The northwest coast of Greenland (drainage zone 8.1) has received much attention due to large mass losses observed in the early twenty first Century (Rignot *et al* 2008, Khan *et al* 2010a). This region of the ice sheet is dominated by vast contact with the ocean—there is very little land, and the ice sheet terminates directly into the ocean. Presently the mass loss is equally split between an SMB anomaly and a discharge anomaly, whereas previous rapid mass loss events were entirely dominated by ice dynamics (Kjær *et al* 2012). Historical aerial photographs from this region show that this region has experienced rapid increases and decreases in discharge (Kjær *et al* 2012), just as has been observed in other regions where the mass loss is heavily affected by oceanic conditions (Howat *et al* 2007, Nick *et al* 2009).

North sector: in contrast to the southwest, Greenland's north sector (drainage basin 1) is characterised by major marine-terminating outlet glaciers. These glaciers are surrounded by year-round sea ice and a thick ice mélange, which appears to suppress calving front retreat (Amundson *et al* 2010, Seale *et al* 2011, Christoffersen *et al* 2012, Schild and Hamilton 2013). Occasionally the sea-ice breaks up, leaving the outlets open to oceanic forcing, which may lead to large calving events (Higgins 1991, Reeh *et al* 2001). The Petermann Glacier is among the largest of the Greenlandic outlets, with the second largest floating shelf (Rignot *et al* 2001). Unlike most other glaciers in Greenland, the majority of the mass loss (~80%) occurs as submarine melt. In 2010 a very large calving event occurred, removing ~25% of the glacier tongue (Falkner

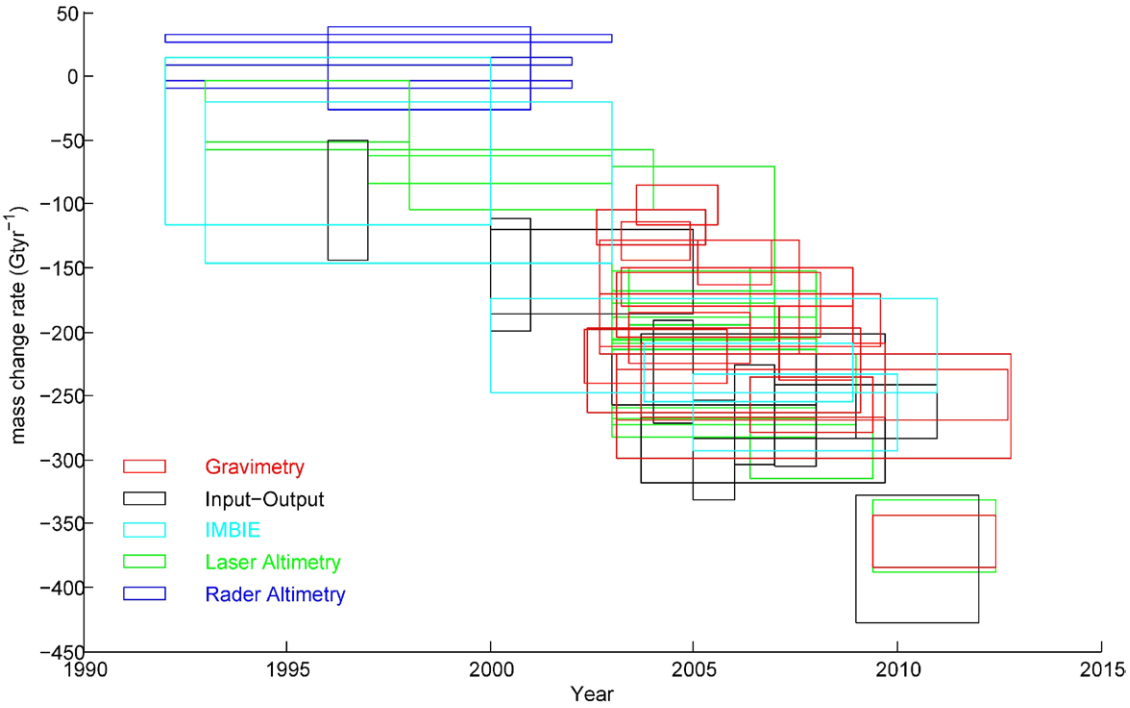

Figure 11. Mass changes during 1992–2012. Colours refer to the different methods used to derive estimates. The *x* and *y* directions of the squares denote the time intervals and uncertainties of the mass loss rate. See table 1 for references.

et al 2011, Nick *et al* 2012). The calving is likely a part of a natural cycle, and did not lead to increased mass loss or speed-up of the ice stream (Falkner *et al* 2011, Nick *et al* 2012). This sector of the ice sheet has a negative SMB anomaly. And while the SMB anomaly has varied throughout the last decade, the discharge component has remained stable (Khan *et al* 2014a).

In the northeast sector (drainage basins 2.1 and 2.2) there have been observations of increased discharge and melting. This sector is occupied by the prominent North East Greenland Ice Stream (NEGIS), which drains into the outlets of the 79 Fjord glacier, Zachariae Isstrøm, Storstrømmen, and Bidstrup Glacier. The former two outlet glaciers have both lost large amounts of ice through increased discharge starting during the period 2003–2006 and continuing into the present (Khan *et al* 2014a).

3.2. Ice-sheet-wide mass changes since 1978

By comparing recent estimates of the GrIS mass balance with those since the early 1990s, its evident that mass loss from the ice sheet has more than doubled during the past quarter of a century (figure 11). Estimates of the state of the GrIS include those derived from space-borne radar altimetry, air-and space-borne laser altimetry, satellite gravimetry, the input–output method, and very often a combination of more than one type of measurement (references are given in table 1). See section 2 for a description of the methods.

The period from the 1990s to the beginning of the twenty-first century was characterised by a relatively small mass loss. At higher elevations above 2000 m the ice sheet was in balance and even thickening, while at lower elevation the periphery was thinning (Krabill *et al* 1999, 2000, Zwally *et al* 2011). During the 1990s the SMB contribution to the mass loss increased, owing to a larger surface melt with precipitation that remained constant. Ice discharge also increased during this period, and total annual mass loss rates of 51 Gt yr^{-1} were reported for the GrIS from 1994 to 1999 (Rignot *et al* 2011).

In northeast and northwest Greenland the observational record was recently extended back to 1978 and 1985, respectively, using aerial stereo-photogrammetric imagery that provided new information on ice dynamics. In northeast Greenland the ice margin remained stable from 1978 until ~2003, at which time the ice loss started to rapidly increase. The ice loss has accelerated continuously since 2003 (Khan *et al* 2014). In northwest Greenland aerial imagery combined with geodetic observations revealed two periods of considerable dynamic-induced ice loss from the ice sheet margin, namely 1985–1993 and 2005–2010, while mass loss during the intervening period was governed by SMB-induced changes (Kjær *et al* 2012, Khan *et al* 2013).

3.3. Long-term mass changes (century timescale)

Modern aerial and satellite observations allow measurements of volume and mass change at various temporal and spatial scales. However, these are confined to recent decades. In recent years several studies have focused on changes in front positions of outlet glaciers during the satellite-era from the 1970s and onwards at various temporal and spatial scales (Moon and Joughin 2008, Box and Decker 2011, Howat and Eddy 2011, McFadden *et al* 2011, Carr *et al* 2013). Mapping the front position over sufficiently long timescales may provide information about the outlet glaciers dynamic response to slowly changing external forcings.

Table 1. Mass loss rates: rate of mass change of the GrIS derived from different methods.

Source and Year	Technique	Time range	Mass loss rate Gt yr^{-1}	Notes
	Radar			
Zwally *et al* (2005)	SRALT (ERS 1–2) + limited ATM	1992–2002	11 ± 3	Satellite radar altimetry is affected by surface slope near ice margins and changes in penetration
Johannessen *et al* (2005)	SRALT (ERS 1–2) low elevations sparsely sampled	1992–2003	30 ± 3	Densities of 0.9, 0.5, 0.4, 0.3, 0.3 Gt km^3 assumed to convert area-weighted height change in elevation into mass intervals (<1.5, 1.5–2, 2–2.5, 2.5–3, >3 km)
Zwally *et al* (2011)	SRALT (ERS 1–2) + limited ATM	1992–2002	−7 ± 3	Superseeds Zwally *et al* (2005)
Hurkmans *et al* (2014)		1996–2001	5.5 ± 32.1	
	Air- and space-borne laser altimetry			
Krabill *et al* (2004)	ATM	1993–1998	−55 ± 3	
		1997–2003	−73 ± 11	
Thomas *et al* (2006)	ATM	1993–1998	−27 ± 24	High end of range likely due to limited coverage at low elevations
	ATM/ICESat	1998–2004	−81 ± 24	High end of range likely due to limited coverage at low elevations
Slobbe *et al* (2009)	ICESat	2003–2007	−139 ± 68	Used large density range (±300 kg m^3) for error bounds
Zwally *et al* (2011)	ICESat	2003–2007	−174 ± 4	
Sørensen *et al* (2011)	ICESat	2003–2008	−233 ± 27	
		2003–2008	−191 ± 23	
		2003–2008	−240 ± 28	
Ewert *et al* (2012)	ICESat	2003–2008	−181 ± 28	
Sasgen *et al* (2012)	ICESat	2003–2009	−245 ± 28	
Khan *et al* (2014a)	ATM + LVIS + ICESat	2003–2006	−172.4 ± 21,7	
		2006–2009	−292 ± 23,2	
		2009–2012	−359.8 ± 28,9	
Hurkmans *et al* (2014)	ICESat	2003–2008	−234.8 ± 46.9	
	Input–Output method			
Rignot and Kanagaratnam (2006)	InSAR (ice motion) 1996 + balance anomaly estimate (Hanna *et al* 2005)	1996–1997	−83 ± 28	
	InSAR (ice motion) 1996 + balance anomaly estimate (Hanna *et al* 2005)	2000–2001	−127 ± 28	
	InSAR (ice motion) 1996 + balance anomaly estimate (Hanna *et al* 2005) (extrapolated)	2005–2006	−205 ± 38	
van den Broeke *et al* (2009)	InSAR-RACMO	2003–2008	−237 ± 20	

(*Continued*)

Table 1. (*Continued*)

Source and Year	Technique	Time range	Mass loss rate Gt yr^{-1}	Notes
Sasgen *et al* (2012)	InSAR-RACMO	2003–2009	−260 ± 58	
Enderlin *et al* (2014)	SMB—D	2000–2005	−153 ± 33	
		2005–2009	−265 ± 18	
		2009–2012	−378 ± 50	
Langer *et al* (2014)	SMB—D	2007–2011	−262 ± 21	
	GRACE			
Chen *et al* (2006)	GRACE—averaging filter applied to monthly spherical harmonic gravity field product	2002–2005	−219 ± 21	
Luthke *et al* (2006)	GRACE MASCON—(change in gravitational acceleration on each orbital pass fit to forward model of mass history of local basins)	2003–2005	−101 ± 16	Gain of 54 Gt yr^{-1} above 2000 m and loss of 155 Gt yr^{-1} below 2000 m
Velicogna and Wahr (2006)	GRACE—averaging filter applied to monthly spherical harmonic gravity field product	2002–2006	−227 ± 33	
Ramillien *et al* (2006)	GRACE—averaging filter applied to 10 d gravity solutions	2002–2005	−118 ± 14	
Wouters *et al* (2008)	GRACE EOF decomposition of monthly spherical harmonics iteratively fit with forward model of mass change of basins (based initially on R&K and iterated)	2003–2008	−179 ± 25	
		2003–2005	−121 ± 27	Same period as Luthke *et al* (2006) similar elevation dependence seen
		2006–2008	−204 ± 25	Range in net balance is range of results using gravity products from four diff erent centers, rather than estimated error
Slobbe *et al* (2009)	GRACE using products from CNES (Centre National d'Etudes Spatiales), CSR (Center for Space Research, University of Texas-Austin), DEOS (Delft Institute of Earth Observation and Space Systems, Delft University of Technology, Delft), and GFZ (GeoForschungsZentrum, Helmholtz-Zentrum Potsdam)	2002–2007	−173 ± 45	Range: −128 to −218 Gt yr^{-1}
Velicogna (2009)	GRACE	2002–2009	−230 ± 33	
Ewert *et al* (2012)	GRACE—GFZ	2002–2009	−191 ± 21	
Sasgen *et al* (2012)	GRACE	2003–2009	−238 ± 29	
Siemes *et al* (2013)	GRACE—DEOS	2003–2004	−129 ± 15	
		2005–2006	−146 ± 17	
		2007–2008	−209 ± 29	
		2003–2008	−165 ± 15	
Barletta *et al* (2013)	GRACE	2003–2011	−234 ± 20	
		2003–2008	−211 ± 23	
		2002–2007	−179 ± 22	
		2007–2011	−276 ± 27	

(*Continued*)

Table 1. (*Continued*)

Source and Year	Technique	Time range	Mass loss rate Gt yr^{-1}	Notes
Velicogna and Wahr (2013)	GRACE	2003–2012	−258 ± 41	
Wouters *et al* (2013)	GRACE	2003–2012	−249 ± 20	
Khan *et al* (2014a)	GRACE	2003–2006	−205 ± 20,2	
		2006–2009	−256.6 ± 21,8	
		2009–2012	−359.8 ± 20,3	
	The ice sheet mass balance inter-comparison exercise (IMBIE)			
Shepherd *et al* (2012)	Reconciled estimate from radar, laser altimetry, input–output, and GRACE	1992–2012	−142 ± 49	
		1992–2000	−51 ± 65	
		1993–2003	−83 ± 63	
		2000–2011	−211 ± 37	
		2005–2010	−263 ± 30	
		2003–2008	−232 ± 23	
	Empirical relations between surface mass balance and ice discharge			
Rignot *et al* (2008)	Regression between SMB-anomalies with ice discharge	1960–1970	−110 ± 70	
		1970–1990	−30 ± 50	
		1996	−97 ± 47	
		2000	−156 ± 44	
		2004	−231 ± 40	
		2005	−293 ± 39	
		2006	−265 ± 39	
		2007	−267 ± 38	
Yang (2011)	Regression between inter-annual anomalies in modeled melt-index and ice discharge estimates from Rignot and Kanagaratnam (2006)	1958–2007	−170 ± 50	
		1961–2003	−167 ± 50	
		1993–2003	−163 ± 47	
		1996–2007	−213 ± 56	
Box and Colgan (2013)	Regression between 13 year smoothed runoff and ice discharge	1840–2010	−52.6 ± 21,0	
	Energy- and climate modeling			
Van de Wal and Oerlemans (1994)	Energy balance modeling	1890–1990	−90 ± 46,8	
Zuo and Oerlemans (1997)	Glacier mass balance and climate modeling	1865–1990	−86.4 ± 25,2	

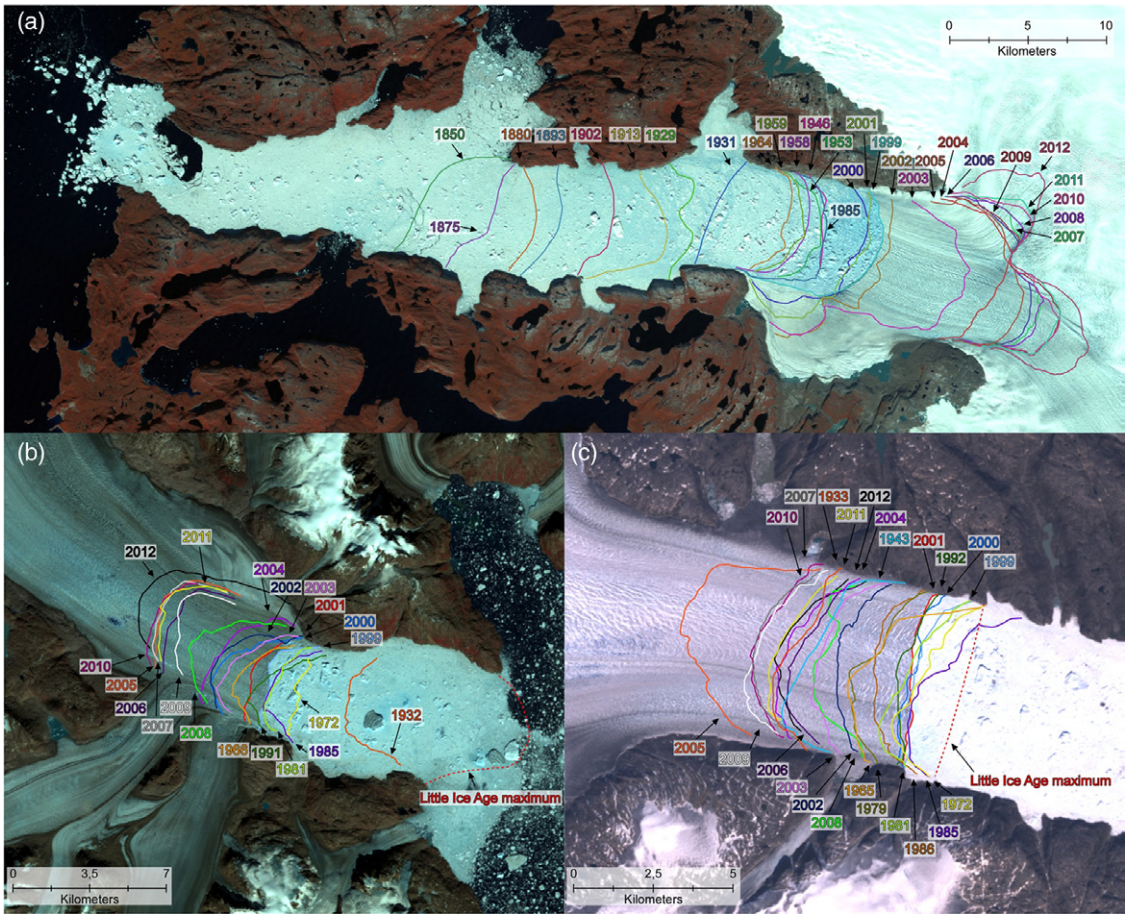

Figure 12. Glacier front positions of Jakobshavn Isbræ (*a*), Kangerdlugssuaq Glacier (*b*), and Helheim Glacier (*c*). Glacier front positions are based on historical maps from early expeditions, aerial imagery from the 1930s and onwards, and satellite observations. The background map is a Landsat7 ETM+ 'true color' image.

To extend the observational record of surface lowering and glacier front positions to the century timescale, back beyond the satellite-era, a range of different methods has been applied. These include the use of historical maps and reports from early expeditions to Greenland during the nineteenth and twentieth centuries, aerial imagery from the 1930s and onwards, and identification of the Little Ice Age extent on contemporary aerial and satellite-imagery (Andresen *et al* 2014, Weidick 1959, 1994, Podlech *et al* 2004, Csatho *et al* 2008, Bjørk *et al* 2012, Kelley *et al* 2012, Lecleqer *et al* 2014, Lea *et al* 2014, Khan *et al* 2014b). The Little Ice Age was a period of cooling that occurred from about 1350 to about 1850. The maximum ice extent during the Little Ice Age is identified using the so-called 'historical moraines', i.e. fresh non-vegetated moraines close to the present glacier fronts seen in many parts of Greenland, and fresh trimlines, i.e. pronounced boundaries between abraded and less-abraded bedrock on valley sides (Csatho *et al* 2008, Khan *et al* 2014b; see also figure 12). These mark the culmination of the Little Ice Age glacier advances.

In general, Greenland outlet glaciers respond rapidly to atmospheric and oceanic forcing. For example warming during the 1920s and 1930s caused retreat of glaciers, while slowing down or even re-advance occurred during the cooler mid-twentieth century (Andresen *et al* 2014, Weidick 1994, Bjørk *et al* 2012). However, despite overall regional trends, adjacent outlet glaciers may have reacted differently during the twentieth century after being subjected to the same external forcing, thus underlining the important impact of bathymetric and topographic control (Andresen *et al* 2014, Warren and Glasser 1992, Weidick 1994, Bjørk *et al* 2012, Kelley *et al* 2012, Enderlin *et al* 2013). An example of this is the inner part of the Nuuk fjord in southwest Greenland, where the marine-terminating glacier Kangia Nunâta Sermia has shown extreme recession, initiated as early as in the 1700s. However, the nearby marine-terminating glacier Narsap Sermia has remained at its Little Ice Age position during the twentieth century, while the land-terminating glacier Saqqap Sermia has advanced during much of the twentieth century (Weidick 1994, Lea *et al* 2014). The different behaviour of marine and land-terminating outlet glaciers has also been identified elsewhere in western Greenland, where Kelley *et al* (2012) found that land-terminating glaciers have retreated less than their marine-terminating counterparts since the Little Ice Age.

The long-term records of ice front positions (see figure 12) provide information on the dynamic behaviour of the outlet glaciers. The variability of the front positions illustrates the importance of obtaining long-term records. A number of studies have assessed the effects of changing air and ocean temperatures on outlet glacier front position, while also considering

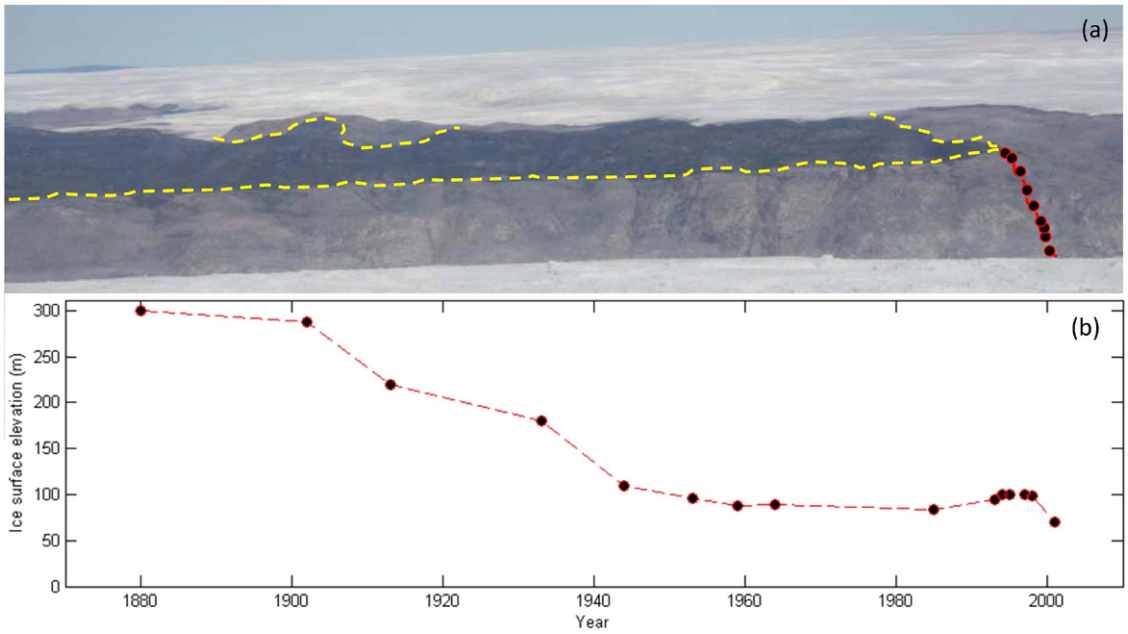

Figure 13. (*a*) Photo from 2013 of the northern margin of Jakobshavn Isbræ in west Greenland. The yellow line denotes the Little Ice Age trim line. The black dots represent the ice surface position shown in the bottom panel. (*b*) The ice surface elevation from photos.

the influence of the topographic setting (Andresen *et al* 2014, Andresen *et al* 2012, Bjørk *et al* 2012, Enderlin *et al* 2013, Khan *et al* 2014b). However, while these studies provide valuable records of long-term variability, they do not include estimates of long-term elevation changes of the outlet glaciers, or of mass balance for the ice sheet.

Analysis of an individual outlet glaciers' behaviour can be undertaken using high-resolution aerial stereo-photogrammetric imagery and digital elevation models, combined with field observations (Weidick 1968, Csatho *et al* 2008, Lea *et al* 2014, Khan *et al* 2014b). Figure 13 shows elevation changes of Jakobshavn Isbræ obtained from the northern rim of the Isfjord, combined with observations from aerial stereo-photogrammetric imagery and airborne laser altimetry. The observations, combined with observed changes in velocity, reveal that the behaviour of Jakobshavn Isbræ represents a complex dynamic response to local climate forcing (Csatho *et al* 2008). Khan *et al* (2014b) examined the long-term response of Kangerdlugssuaq Glacier and Helheim Glacier in southeast Greenland, and found that Kangerdlugssuaq Glacier experienced substantial lowering (230–265 m) and frontal retreat between the early 1930s and 1981. In contrast, Helheim Glacier experienced only limited net thinning and frontal retreat. Aerial imagery of Helheim Glacier from the 1930s and onwards show that the glacier front has retreated and re-advanced on multiple occasions, revealing that Helheim Glacier experienced several periods of dynamic thinning and thickening. The overall elevation change from the early 1930s to 1981 is close to zero (Bjørk *et al* 2012, Khan *et al* 2014b). Records of glacier front positions and elevation changes of Jakobshavn Isbræ, Kangerdlugssuaq Glacier, and Helheim Glacier suggest a complex long-term behaviour, which is not always captured by ice sheet models (Csatho *et al* 2008, Khan *et al* 2014b).

While the GrIS mass balance during the past decades have been studied using a range of aerial and satellite observations extending back to 1992, long-term records before the early 1990s are limited. Figure 14 and table 1 show the different methods for assessing estimates of change and the timescales of the observations.

A number of recent efforts to model past atmospheric conditions over the GrIS, use output from long-term global atmospheric models as boundary conditions to force regional atmospheric circulation models. One suite of useful long-term global models is provided by the European Centre for Medium-Range Weather Forecasts (ECMWF) re-analysis project. The output from the global ECMWF re-analysis model covers September 1957–2002. There is also an updated ECMWF re-analysis Interim data set, which spans 1979 to the present. Thus, estimates of the GrIS mass balance that rely on ECMWF reanalysis data as input to determine the SMB of the ice sheet, extend back only to 1958.

Rignot *et al* (2008) provided a continual time series of the GrIS mass balance from 1958 onwards, that was based on an empirical relationship between 3 year-smoothed SMB-anomalies and ice discharge. They showed that during the 1960s the ice sheet was losing mass (at a rate of 110 ± 70 Gt yr^{-1}), and that the ice sheet was in near balance during the 1970s and 1980s (30 ± 50 Gt yr^{-1}); while from the 1990s and onwards the mass loss rate increased (1996: 97 ± 47 Gt yr^{-1}; 2007: 267 ± 38 Gt yr^{-1}), in accordance with other studies. Yang (2011) used an empirical melt sensitivity model to reconstruct the ice discharge, and arrived at a total mass loss rate of 170 ± 50 Gt yr^{-1} during 1958–2007 (see figure 14).

A longer record of mass balance change is provided by Box and Colgan (2013) who used ice core records and temperature reconstructions combined with regional climate model output to obtain a SMB time series from 1840 to the present. Using basically the same method as Rignot *et al* (2008), Box and Colgan (2013) generated a reconstruction of the mass balance which was scaled using independent GRACE observations

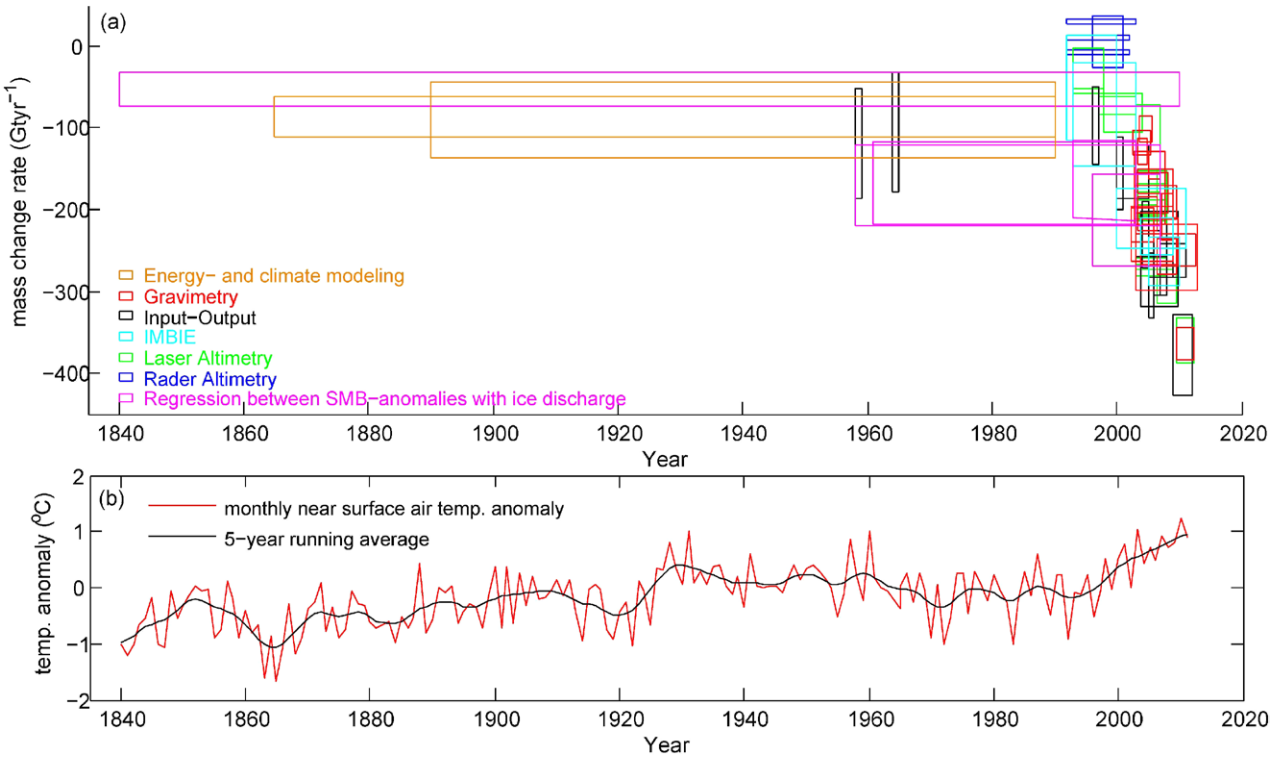

Figure 14. (*a*) Mass changes during 1840–2012. Colours refer to the different methods used to derive estimates. See table 1 for references. (*b*) The lower panel is the Greenland-wide near-surface air temperature anomaly updated from Box *et al* (2009). The solid red line denotes a 5 year running average.

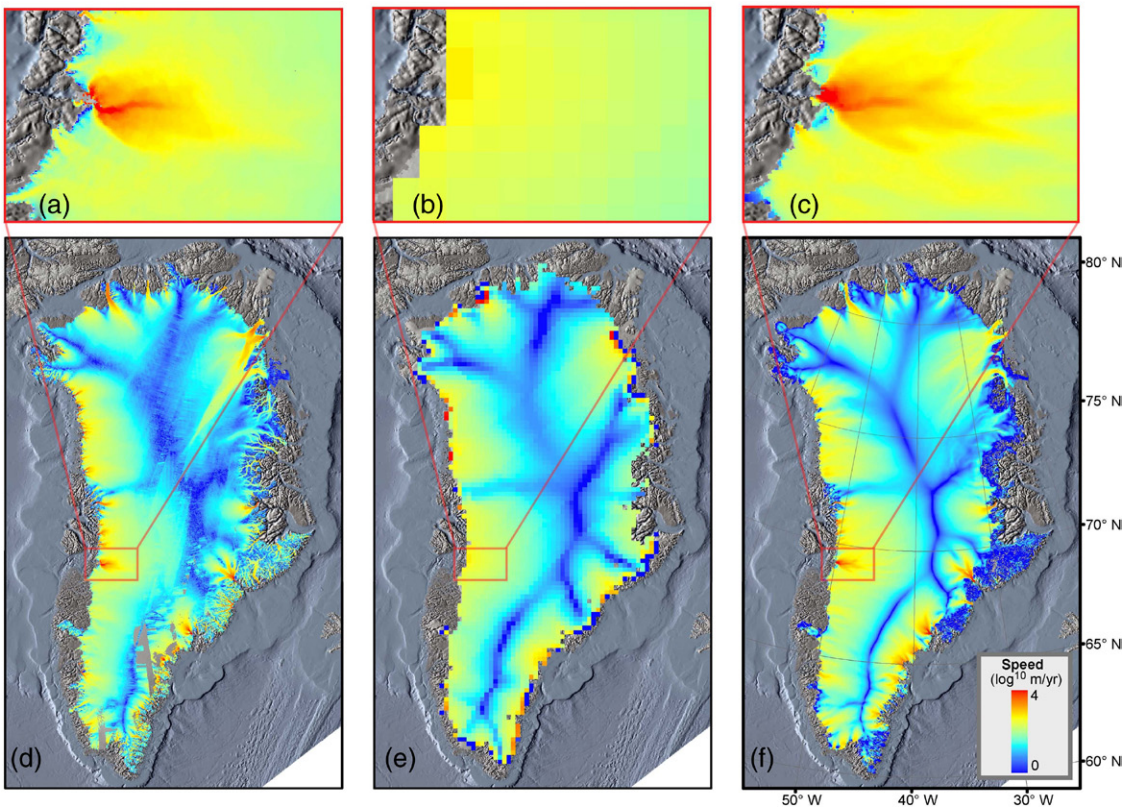

Figure 15. Illustration of advances in ice sheet modelling since AR4 (IPCC 2007). (*a*) and (*d*) Observed surface speeds from Joughin *et al* (2010).(*b*) and (*e*) A model simulation using model physics and forcings available prior to AR4. (*c*) and (*f*) A model simulation using model physics and forcings available in 2014. It is important to note that this simulation did not use observed surface velocities during data assimilation. (*a*), (*b*) and (*c*) show zoom over Jakobshavn Isbræ.

(Box and Colgan also preferred parameterizing the ice discharge in terms of the 13 year smoothed runoff, rather than the 3 year smoothed SMB anomaly used by Rignot *et al* (2008). Box and Colgan (2013) found a total mass loss rate of 53 ± 21 Gt yr^{-1} during 1840–2010 (equivalent to a total sea level contribution of 2.5 ± 1.0 cm). Furthermore, their reconstruction showed considerable inter-decadal variability in the mass balance, yielding an ice sheet that was in near balance, even slightly positive, during the second half of the nineteenth century, while during the twentieth century their reconstruction revealed periods of considerable mass loss during 1920–mid-1930s, 1950–1970, and 2000–2010, and a positive mass balance during 1970–2000.

Alternative methods for estimating the mass balance change of the GrIS stem from sensitivity analysis to climate change and energy balance modelling. For example Zuo and Oerlemans (1997) modelled glacier mass balance sensitivity to climate change and historical temperature data and estimated a mass loss rate of 86 ± 25 Gt yr^{-1} (equivalent to a total sea level contribution of 2.7 ± 0.9 cm) during 1865–1990. This is consistent with van de Wal and Oerlemans (1994) who, based on calculations with an energy balance model, estimated a GrIS mass loss rate of 90 ± 47 Gt yr^{-1} (given in sea-level equivalents 2.5 ± 1.3 cm) between 1890 and 1990.

4. Sensitivity to external forcing

Mass loss from the GrIS is regionally distributed between sectors that exhibit different sensitivities to external forcing. Enhanced surface melting and speedup of glacier flow dominate the mass loss in the southeast, west, northwest and northeast parts of the GrIS, where most of the ice margin is in contact with the ocean. Here, the ice-ocean interface plays an important role, as warm oceans currents can significantly increase the melt rate at the glacier termini. Observations over the past two decades show that a speeding up of the many tidewater glaciers coincides with the entry of warmer waters into the fjord systems, enabling rapid retreat of the termini (Holland *et al* 2008, Murray *et al* 2010, Straneo *et al* 2010, 2012). Additionally, the rate of submarine melting is governed by the subglacial freshwater discharge (water that flows through channels at the glacier bed) from the grounding zone, as this drives the circulation of warm seawater that is brought into contact with the ice face through buoyancy-driven convection (Rignot *et al* 2010, Motyka *et al* 2011, Enderlin and Howat 2013). Furthermore, warmer water may reduce ice mélange in glacier fjords. Especially during winter, a reduction of ice in the fjord may result in higher than average-winter speed and lengthening of the duration of the high rate of iceberg production (calving) (Amundson *et al* 2010).

Both models and observations suggest that the speed up of, for example, Helheim, Kangerdlugssuaq, Jakobshavn, Upernavik, and Zachariae Isstrøm are responses to the retreat of the termini (Howat *et al* 2007, Price *et al* 2011, Khan *et al* 2013, 2014a, Nick *et al* 2013). The retreat reduces downstream resistive stresses, which are redistributed upstream. A bed that slopes down inland may lead to unstable grounding-line retreat, as increased flux and consequently reduced buttressing leads to thinning and eventual flotation of the glacier front, which makes the grounding line migrate inland into greater depths of the bed. Kangerdlugssuaq, Jakobshavn, and Zachariae Isstrøm possess a negative bed slope (Joughin *et al* 2012, Bamber 2013a, Khan *et al* 2014b) that lies below sea level, the key condition for satisfying the marine ice sheet instability hypothesis associated with parts of west Antarctica (Weertman 1974, Mercer 1978, Thomas 1979, Schoof 2007, Joughin *et al* 2014b). All three glaciers have retreated more than ~10 km during the last decade and continue to undergo dynamic thinning.

The shape of the outlet (i.e. bed elevation and width) is an important factor that can dominate glacier dynamics (Pfeffer 2007). A sensitivity study by Enderlin *et al* (2013) suggests that for glaciers with similar ice discharge, the trunks of wider glaciers and those grounded over deeper basal depressions tend to be closer to flotation, so that smaller amounts of dynamically induced thinning can result in rapid, unstable retreat following a perturbation. Therefore, glaciers that are subjected to similar external forcings may react quite differently. For example, Upernavik Isstrøm located in northwest Greenland consists of several outlets that retreated and thinned at different time intervals although they experienced the same external ocean and atmospheric forcings (Khan *et al* 2013). Additionally, the configuration of fjord bathymetry (e.g. the presence of sills and higher submerged plateaus) may have an effect on the exposure of the calving front to different layers in the water column (Andresen *et al* 2014).

The majority of the marine-terminating outlet glaciers in north Greenland are surrounded by year-round sea ice. Sea ice may resistive force that prevents the calving front from rotating and breaking off, reducing the calving rate and temporarily stabilizing the terminus (Amundson *et al* 2010, Nick *et al* 2012). Sea ice extent is typically maximum in March and minimum in September. In South Greenland, most coastal areas are free of sea ice between spring and autumn. However, fluctuation in sea ice concentration can have an effect on calving activities and flow speed near the terminus of a glacier. For example, the speed-up and breakup of Jakobshavn Isbræ's ice tongue in 1998 coincided with a period of reduced sea-ice concentration in nearby Diskobugten (Joughin *et al* 2008a). Similarly, Zachariae Isstrøm in north Greenland is surrounded by year-round sea ice. However, the breakup of Zachariae Isstrøm's ice tongue during 2002–2003 coincided with the absence of sea ice in the glacier fjord in September 2002 and 2003. Sea ice extent depends on, for example, atmospheric pressure, wind intensification, and air temperature. Over past decades, the number of storms and the air temperature in the arctic have increased, resulting in rapidly shrinking sea ice cover (Wang *et al* 2009, Screen *et al* 2011, Stroeve *et al* 2012).

Studies of the ice sheet's land-terminating glaciers (Zwally *et al* 2002, Bartholomew *et al* 2012, Palmer *et al* 2011, Sundal *et al* 2011) and marine terminating outlet glaciers (Joughin *et al* 2008b, Shepherd *et al* 2009, Andersen *et al* 2010) suggest that short-term speedups of ice flow are partially controlled by supraglacial streams and lakes that drain through moulins, and provide meltwater into subglacial environments that increases

basal sliding. Though, a recent study by Schoof (2010) suggests that it is not simply the mean surface melt but the water input variability that is the main driver of short-term glacier velocity increases. Glacier sliding responds to melt indirectly through changes in basal water pressure.

Ice loss due to fluctuations in surface processes shows huge inter-annual and annual variability (van den Broeke *et al* 2009, Tedesco *et al* 2013). Over the last decade, melt and run off have significantly increased (van den Broeke *et al* 2009), resulting in a sustained increase of the ice mass loss rate. Melting records from 2010 and 2012 have especially shown that small fluctuations in, for example, the length of the melt season can more than double the SMB component of ice mass change, suggesting that both short- and long-term atmospheric forcing play an important role in the total mass budget. A study by Hanna *et al* (2014) suggests the recent years of warming are due to warm southerly winds over the western flank of the ice sheet, forming a 'heat dome' over Greenland and leading to the higher air temperatures. The above-normal, near-surface air temperatures observed during the 2010 melt record contribute to accelerated snowpack metamorphism and premature bare ice exposure, rapidly reducing the surface albedo (Tedesco *et al* 2011, Box *et al* 2012), resulting in widespread melting.

5. Recent advances in ice-sheet modelling

Glacier ice is a viscous non-Newtonian fluid—its flow is well-described by the Stokes equations known since the mid-nineteenth century. Challenges arise from specifying boundary conditions, especially at the ice sheet's interface with the lithosphere and the ocean (Vaughan and Arthern 2007).

Since the first thermomechanically-coupled ice sheet model was applied to the Greenland ice sheet in the late 1970s, numerical models have become important tools for studying the response of ice sheets to changes in environmental forcings. However, the inability of models constructed prior to 2007 to track observed rapid changes in Greenland's outlet glaciers, led the Intergovernmental Panel on Climate Change (IPCC) to exclude results from ice sheet models for their Forth Assessment Report (AR4) (IPCC 2007). This boosted model development, entailing significant improvements since AR4 was published.

First, early ice sheet models employed the 'shallow ice approximation' (Hutter 1983), that assumes flow is caused only by vertical gradients in shearing. Recent models implement a more complete representation of flow physics than the AR4 models. Most models now include horizontal stress gradients, though they differ in their treatment of longitudinal coupling. Hybrid models combine the shallow ice approximation for shearing in grounded ice, with the use of membrane stresses in ice shelves and areas of rapid sliding (Bueler and Brown 2009). Models in this category achieve a good compromise between accuracy and computational costs. Higher-order models (Blatter 1995) assume that pressure is determined by ice overburden pressure (the hydrostatic assumption) and ignore horizontal derivatives of the vertical velocity. Solving the Stokes equations without relying on simplifying assumptions is most accurate, but is computationally most demanding. Some ice sheet models can be configured with various stress-balance solvers (Larour *et al* 2012a, Brinkerhoff and Johnson 2013), allowing the choice of the most suitable approximation for the problem at hand. A novel approach that tries to balance computational efficiency with physical accuracy, is to vary the order of model complexity over the modelling domain (Seroussi *et al* 2012) such that the Stokes equations are only solved in areas where they are needed. Thanks to code parallelisation and advanced meshing techniques, century-scale prognostic simulations have become feasible using both higher-order (Brinkerhoff and Johnson 2013) and Stokes (Gillet-Chaulet *et al* 2012, Larour *et al* 2012a, Seddik *et al* 2012) models. However, longer integration times remain prohibitive due to large computational costs. Ice sheet models have also seen improvements in the way phase-changes are handled within temperate ice (i.e. ice at the pressure-melting point). Conventional temperature-based 'cold-ice' models are not energy conserving when temperate ice is present, as changes in the latent heat content in temperate ice are not reflected in the temperature state variable (Aschwanden *et al* 2012). Polythermal models, based on mixture theory, account for the latent heat content within temperate ice, thereby conserving energy. Among polythermal schemes, enthalpy-based formulations provide a unified treatment of conservation of energy for intra-, supra- and subglacial liquid water that is easy to implement into ice sheet models (Aschwanden *et al* 2012, Brinkerhoff and Johnson 2013, Seroussi *et al* 2013).

The predictive skill of a model, however, not only depends on model physics but also on the fidelity of the numerical implementation and the quality of data available for validation (Vaughan and Arthern 2007, Blatter *et al* 2011). Verification (i.e. the comparison of results from a numerical approximation to exact solutions of the same continuum model equations) has become an integral part of model development. A constantly-growing number of analytical solutions suitable for verification (Bueler *et al* 2005, 2007, Leng *et al* 2013, Bueler 2014) provides a partial alternative to hard-to-interpret intercomparison results (Bueler 2014), such as in Pattyn *et al* (2012). In engineering, validation is commonly defined as the process of comparing model results to a set of observations adequate to falsify a model (Roache 1998). Such validation is challenging to apply in ice sheet modelling; nonetheless attempts have been made (Robison *et al* 2010, Burton *et al* 2012). Direct validation of substantial sub-systems such as basal hydrology, thermodynamics, and ice dynamics is difficult or impossible as most or all observations available for validation are not linked to a single process, but are the consequence of a complex interplay between sub-systems. Alternatively, a model's predictive skill can be assessed, at least in part, by forcing a model with known or closely-estimated inputs for past events to see how well the output matches observations (hindcasting). For validation, spatially dense time series of observations are preferred metrics (Aschwanden *et al* 2013).

Second, a model is only as good as its initial conditions and time-dependent boundary forcing (Blatter *et al* 2011). In simple terms, the ice sheet model's task is to redistribute mass gain and loss at its upper and lower surfaces compatible with our

understanding of ice sheet dynamics. Mass flux calculations are most sensitive to errors in ice thickness (or, equivalently, basal topography) (Larour *et al* 2012b), and it is the basal topography beneath the GrIS that controls the flow of ice and its discharge into the ocean (Morlighem *et al* 2014). While ice thickness data have been gathered from airborne radar echo soundings since the 1970s, data acquisition has been skyrocketing since 2009 thanks to NASA's mission Operation IceBridge, thereby vastly improving our picture of Greenland's basal topography, including the discovery of a mega canyon beneath the central GrIS (Bamber *et al* 2013b). To be useful for ice sheet models, sparse ice thickness measurements must be interpolated onto regular or irregular grids. Conventional geostatistical methods such as kriging (Bamber *et al* 2013a) lead to large errors in flux divergence (Morlighem *et al* 2013). This poses a fundamental limitation to ice sheet models, as unphysically large flux divergences force the ice sheet model to redistribute mass in order to reconcile topography and ice flow, and potentially converging to a steady state that is significantly different from the initial condition (Seroussi *et al* 2011). In fast flowing areas, errors in flux divergence can be greatly reduced by combining the sparse radar data with high-resolution flow measurements via mass conservation (MC; Morlighem *et al* 2013). An application of MC revealed deep submarine valleys aligned with fast flow features in Greenland (Morlighem *et al* 2014).

Next, Greenland's marine-terminating glaciers are sensitive, and respond rapidly, to oceanic perturbations (Howat *et al* 2007, Holland *et al* 2008, Nick *et al* 2009, Murray *et al* 2010). Processes in the vicinity of the ice sheet's interface with the ocean are complex, acting on a multitude of spatial and temporal scales, and (so far) prohibiting a unified theory. Numerical flow-line studies suggest that the thinning-induced change in basal effective pressure is the dominant process influencing near-terminus behaviour (Joughin *et al* 2012). Whole-ice-sheet models now show promise of being able to track the past two decades of observed outlet glacier changes (Price *et al* 2011). New theoretical work on calving, damage mechanics, and grounding line stability (Pralong and Funk 2005, Benn *et al* 2007, Schoof 2007, Amundson and Truffer 2010, Bassis 2011) is informing model development. Ice sheet models now implement first-order kinematic calving laws (Levermann *et al* 2012) as well as fracture/damage mechanics (Albrecht and Levermann 2012, Borstad *et al* 2012, Albrecht and Levermann 2014).

Finally, responding to the call for transparency in science and reproducibility of scientific findings (Nielsen 2011), open-source models are becoming increasingly popular. Ice sheet models capable of high-resolution, century-scale prognostic simulations that are open source include Elmer/Ice (Gagliardini *et al* 2013), the Ice Sheet System Model (ISSM; Larour *et al* 2012a), the Parallel Ice Sheet Model (PISM; www.psim-docs.org), and the Variational Glacier Simulator (VarGlas; Brinkerhoff and Johnson 2013).

5.1. Challenges and outlook

Boundary conditions such as the bed's stress and thermal state, are intrinsically difficult, if not impossible, to measure. Basal stresses, for example, can vary spatially and temporally by orders of magnitude and can depend strongly on local basal hydraulics, while measuring basal motion is difficult, expensive, and usually limited to a few isolated points (Greve and Blatter 2009). Despite decades of intensive research, no unifying theory of how basal stresses relate to basal motion is yet available. A high geothermal flux can locally raise the basal temperature to the pressure-dependent melting point, thereby initiating sliding. To make matters worse, heat flow is heterogeneous and can vary on scales of less than 100 km (Dahl-Jensen *et al* 2003, Näslund *et al* 2005). So far, few direct measurements of heat flux exist (Fahnestock *et al* 2001), and indirect methods (Shapiro and Ritzwoller 2004, Fox Maule *et al* 2005) have limited accuracy (Alley and Joughin 2012). While the exponential dependence of ice viscosity on temperature is reasonably well-constrained by measurements, high shear rates near the bed result in strongly anisotropic flow characteristics. At the pressure melting point, additional ice softening occurs due to the presence of liquid water (Duval 1977), though this relationship remains poorly quantified (Duval 1977, Lliboutry and Duval 1985).

It has become evident that variations in surface melting affect not only the flow speed of mountain glaciers (Iken 1978, 1981), but also near-coastal areas of the GrIS (Zwally *et al* 2002, Das *et al* 2008, Palmer *et al* 2011). The impact of these fluctuations on the GrIS in a warming climate has not yet been quantified (Sundal *et al* 2011). Recent theoretical and numerical studies (Schoof 2010, Hewitt 2011, Werder *et al* 2013, de Fleurian *et al* 2014) on idealised geometries and mountain glaciers are guiding the development of numerical subglacial hydrology models applicable to the GrIS (Bueler and Pelt 2014). However, any such model has a necessarily large number of parameters for which none or few observational constraints yet exist, making comprehensive parameter sensitivity studies indispensable. In addition, basal hydrology models are computationally expensive because water movement in the subglacial aquifer is fast compared to the flow of the overlying ice, and numerical schemes must choose small time steps accordingly.

As observations alone are insufficient to provide the initial conditions for prognostic ice sheet models, data assimilation techniques must be combined with parameterisations of processes to provide the necessary initial and boundary conditions. Reconstruction of basal properties using inverse methods has become an integral part of ice sheet modelling. High-resolution surface velocity is the most commonly used observable in the assimilation process, but recent work by Larour *et al* (2014) also includes time-dependent surface altimetry data. Remaining inconsistencies in initial conditions cause large flux divergences that result in transient signals propagating through the system at the beginning of the run (Gillet-Chaulet *et al* 2012, Brinkerhoff and Johnson 2013). Also, the parameter fields resulting from inversion may not be applicable for prognostic simulations, as these parameters evolve with time (Aschwanden *et al* 2013). Ideally, inverse methods are applied to recover material properties, such as till friction angle, and the connection to time-evolving basal drag should be made by subglacial hydrology models. Initialising

ice sheet models is challenging; the initial state needs to be close to the currently-observed ice sheet, including the temperature field, while at the same time remaining fully self-consistent with climate forcing in order to minimise unnatural transients in the model response, but also maintain the natural response of the model which results from its initial state (Aðdalgeirsdóttir *et al* 2014).

Model simulations prepared for the Fifth Assessment Report (Vaughan 2013) of the IPCC suggest that over the next two centuries the evolution of the GrIS will most likely be dominated by uncertainties in future SMB (Bindschadler *et al* 2013, Nowicki *et al* 2013), though the recently discovered presence of deep, widespread submarine glacial valleys around Greenland implies that Greenland outlet glaciers remain the wild card (Morlighem *et al* 2014). Accurate modelling of SMB relies on realistic simulation of local climate, snow processes, albedo evolution, refreezing, and adequate horizontal resolution to capture high SMB gradients at ice sheet margins (Vizcaíno 2014). To capture the SMB elevation feedback, ice sheet models need to be directly coupled to general or regional circulation models. A core requirement of successful two-way coupling is the conservative exchange of mass and energy fluxes between the models (Fischer *et al* 2014). The first realistic results of fully-coupled models are now emerging (Vizcaíno *et al* 2013, 2014, Fyke *et al* 2014). Alternatively, parameterisations of SMB changes have been proposed (Helsen *et al* 2012, Franco *et al* 2012, Edwards *et al* 2014a) and tested (Edwards *et al* 2014b).

Substantial challenges also remain where the ice is in contact with the ocean. Furthering our understanding of ocean-induced ice sheet melting is currently hampered by the logistical difficulties of observational studies (Joughin *et al* 2012), and the early developmental state of coupled high-resolution, ocean-ice sheet models.

6. Concluding remarks

Mass loss from the GrIS is a complex function of processes related to SMB and ice dynamics, forced mainly by short- and long-term fluctuations in the atmospheric and oceanic energy input. Measurements from combining satellite altimetry, airborne altimetry, interferometry, and gravimetry data sets over the last decade show a doubling of the ice loss rate due to a combination of increased ice discharge and SMB-inferred mass change (Pritchard *et al* 2009, van den Broeke *et al* 2009, Moon *et al* 2012). Khan *et al* (2014), for example, obtained an ice loss rate of 172.4 ± 21.7 Gt yr^{-1} during 2003–2006 and 359.8 ± 28.9 during 2009–2012. However, the trend from 2003–2012 was 274 ± 24 Gt yr^{-1} (see table 1), with an approximately equal split between surface processes and ice dynamics. Studies using airborne laser altimetry, satellite radar altimetry, and the input–output method suggest a much lower mass loss rate of 50–100 Gt yr^{-1} in the 90s (see table 1). Extending the record back to 1840 suggests a long-term mass loss rate of 50–90 Gt yr^{-1} over the last century (see figure 14). During the twentieth century the rate of mass change was highly variable with a much higher mass loss rate during the warming in the 1920s and 1930s, while the ice sheet was near balance during the 1970s and 1980s (Rignot *et al* 2008, Box and Colgan 2013). The variability is also clear from historical aerial images combined with both early and modern satellite imagery covering outlet glaciers. These data sets allow long-term mapping of the glacier front positions, and thus permit indirect evaluations of ice discharge. From extensive spatial coverage, it is also clear that different outlet glaciers can react differently to comparable external atmospheric and oceanic forcings. This suggests that other factors, such as the shape of the glacier outlet and the fjord bathymetry, are important components for determining the short- and long-term behaviour of the glaciers.

One of the major questions regarding the future stability of the GrIS, is whether the mass loss will continue to accelerate as air and ocean temperatures increase. Recent mapping of the subglacial topography (Morlighem *et al* 2014) has shown Greenland to possess much larger deep, incised, subglacial fjords than previously thought. Those features are believed to amplify the acceleration of ice discharge.

Ice sheet modelling has come a long way since the publication of AR4, and even more so since the first application of an ice sheet model to the GrIS. Ice sheet models have seen key improvements in the way they handle stresses and the thermal state within the ice. Better representation of marginal processes and increased grid resolution is facilitating the tracking of changes in outlet glaciers and their marine termini. However, no ice sheet model has demonstrated sufficient skill in hindcasting the evolution of the Greenland ice sheet during the past decades; until then model-based century-scale sea-level projections should be taken with a grain of salt. Some of the issues, while being far from trivial, are no road blocks on the path to progress. Within a decade model coupling techniques will mature sufficiently for ice sheets to become a standard part of Earth System Models, capturing feedbacks between all the physical systems involved. Thanks to the ever-increasing availability of high-performance computing systems, fully-coupled simulations will be feasible at grid resolutions sufficient to resolve the high gradients in surface mass balance and the changes in fast flow in outlet glaciers. Model coupling must be complemented by innovative approaches to model initialization. Targeted observations, especially at the lateral and basal boundary, will reduce uncertainties in boundary conditions, provide valuable input for model validation, and further our process understanding. These observations will also help answering whether Stokes models are warranted or computationally-efficient lower-order approximations are sufficiently accurate for sea-level predictions. As suggested by Vaughan and Arthern (2007), we will perform ice sheet forecasts similarly to weather forecasts where suites of models are continuously run with different initial conditions. These efforts are to be accompanied by rigorous formal sensitivity analyses to assess uncertainty propagation. Furthermore we will quantify the time scale when ice sheet weather turns into ice sheet climate. Despite all anticipated progress, major obstacles in the quest for better sea-level predictions are, and will remain, our limited understanding of the physical processes at the ice-ocean interface and the lack of a prognostic

sliding law. The challenges here are multifold. First, measurements where the ice meets the ocean are inherently difficult and the bottom of an ice sheet will remain largely inaccessible. Next, it is unclear if the currently-observed quantities are sufficient to characterise the physical processes we are trying to understand. Are there quantities we could measure additionally that would facilitate progress? Last, we must cast our process understanding into a set of equations that can be solved numerically. A 'grand string theory' of glaciology spanning across temporal and spatial scales is unlikely to emerge in the next decade; instead smaller and larger pieces will have to be laboriously put together like a jigsaw puzzle. Of course good things don't come easy, and all good things take some time. Substantial progress can only arise from a concerted community effort in which ice sheet modellers have become well-integrated within the broader climate modelling community.

References

Aðalgeirsdóttir G, Aschwanden A, Khroulev C, Bomberg F, Mottram R, Lucas-Picher P and Christensen J H 2014 Role of model initialization for projections of 21st-century Greenland ice sheet mass loss *J. Glaciol.* **60** 782–94

Albrecht T and Levermann A 2012 Fracture field for large-scale ice dynamics *J. Glaciol.* **58** 165–76

Albrecht T and Levermann A 2014 Fracture-induced softening for large-scale ice dynamics *Cryosphere* **8** 587–605

Alley R B and Joughin I 2012 Modeling ice-sheet flow *Science* **336** 551–2

Amundson J M, Fahnestock M, Truffer M, Brown J, Lüthi M P and Motyka R J 2010 Ice mélange dynamics and implications for terminus stability, Jakobshavn Isbræ, Greenland *J. Geophys. Res.* **115** F01005

Amundson J M and Truffer M 2010 A unifying framework for iceberg-calving models *J. Glaciol.* **56** 822–30

Andersen M L *et al* 2010 Spatial and temporal melt variability at Helheim Glacier, East Greenland, and its effect on ice dynamics *J. Geophys. Res.* **115** F04041

Andresen C S *et al* 2012 Rapid response of Helheim Glacier in Greenland to climate variability over the past century *Nat. Geosci.* **5** 37–41

Andresen C S, Kjeldsen K K, Harden B, Nørgaard-Pedersen N and Kjær K 2014 Outlet glacier dynamics and bathymetry at Upernavik Isstrøm and Upernavik Isfjord, North-West Greenland *Geol. Survey Denmark Greenland Bull.* **31** 81–4

Andersen *et al* 2015 Basin-scale partitioning of Greenland ice sheet mass balance components (2007–2011) *Earth Planet. Sci. Lett.* **409** 89–95

Aschwanden A, Bueler E, Khroulev C and Blatter H 2012 An enthalpy formulation for glaciers and ice sheets *J. Glaciol.* **58** 441–57

Aschwanden A, Aðalgeirsdóttir G and Khroulev C 2013 Hindcasting to measure ice sheet model sensitivity to initial states *Cryosphere* **7** 1083–93

Bamber J L *et al* 2013a A new bed elevation dataset for Greenland *Cryosphere* **7** 499–510

Bamber J L, Siegert M J, Griggs J A, Marshall S J and Spada G 2013b Paleofluvial mega-canyon beneath the Central Greenland ice sheet *Science* **341** 997–9

Barletta V R, Sørensen L S and Forsberg R 2013 Scatter of mass changes estimates at basin scale for Greenland and Antarctica *Cryosphere* **7** 1411–32

Bartholomew I, Nienow P, Sole A, Mair D, Cowton T and King M A 2012 Short-term variability in Greenland ice sheet motion forced by time-varying meltwater drainage: implications for the relationship between subglacial drainage system behavior and ice velocity *J. Geophys. Res.* **117** F03002

Bassis J N 2011 The statistical physics of iceberg calving and the emergence of universal calving laws *J. Glaciol.* **57** 3–16

Benn D I, Warren C R and Mottram R H 2007 Calving processes and the dynamics of calving glaciers *Earth-Science Reviews* **82** 143–79

Bevan S L, Luckman A J and Murray T 2012 Glacier dynamics over the last quarter of a century at Helheim, Kangerdlugssuaq and 14 other major Greenland outlet glaciers *Cryosphere* **6** 923–37

Bevis M *et al* 2012 Bedrock displacements in Greenland manifest ice mass variations, climate cycles and climate change *Proc. Natl Acad. Sci.* **109** 11944–8

Bindschadler R A *et al* 2013 Ice-sheet model sensitivities to environmental forcing and their use in projecting future sea level (the SeaRISE project) *J. Glaciol.* **59** 195–224

Bjørk A A *et al* 2012 An aerial view of 80 years of climate-related glacier fluctuations in southeast Greenland *Nat. Geosci.* **5** 427–32

Blatter H 1995 Velocity and stress fields in grounded glaciers: a simple algorithm for including deviatoric stress gradients *J. Glaciol.* **41** 333–44

Blatter H, Greve R and Abe-Ouchi A 2011 Present state and prospects of ice sheet and glacier modelling *Surv. Geophys.* **32** 555–83

Borsa A A, Moholdt G, Fricker H A, Brunt K M 2014 A range correction for ICESat and its potential impact on ice-sheet mass balance studies *Cryosphere* **8** 345–57

Borstad C P, Khazendar A, Larour E, Morlighem M, Rignot E, Schodlok M P and Seroussi H 2012 A damage mechanics assessment of the Larsen B ice shelf prior to collapse: toward a physically based calving law *Geophys. Res. Lett.* **39** L18502

Box J E 2013 Greenland ice sheet mass balance reconstruction. Part II: surface mass balance (1840–2010) *J. Clim.* **26** 6974–89

Box J E *et al* 2013 Greenland ice sheet mass balance reconstruction. Part I: net snow accumulation (1600–2009) *J. Climate* **26** 3919–34

Box J E and Colgan W 2013 Greenland ice sheet mass balance reconstruction. Part III: marine ice loss and total mass balance (1840–2010) *J. Climate* **26** 6990–7002

Box J E and Decker D T 2011 Greenland marine-terminating glacier area changes: 2000–2010 *Ann. Glaciol.* **52** 91–8

Box J E, Fettweis X, Stroeve J C, Tedesco M, Hall D K and Steffen K 2012 Greenland ice sheet albedo feedback: thermodynamics and atmospheric drivers *Cryosphere* **6** 821–39

Box J E, Yang L, Bromwich D H and Bai L-S 2009 Greenland ice sheet surface air temperature variability: 1840–2007 *J. Clim.* **22** 4029–49

Brinkerhoff D J and Johnson J V 2013 Data assimilation and prognostic whole ice sheet modelling with the variationally derived, higher order, open source, and fully parallel ice sheet model VarGlaS *Cryosphere* **7** 1161–84

Bueler E and Pelt W V 2014 Mass-conserving subglacial hydrology in the Parallel Ice Sheet Model *Geosci Model Dev. Discuss.* **7** 4705–75

Bueler E 2014 An exact solution for a steady, flow-line marine ice sheet *J. Glaciol.* **60** 1117–25

Bueler E and Brown J 2009 Shallow shelf approximation as a 'sliding law' in a thermomechanically coupled ice sheet model *J. Geophys. Res.* **114** F03008

Bueler E, Brown J and Lingle C S 2007 Exact solutions to the thermomechanically coupled shallow-ice approximation: effective tools for verification *J. Glaciol.* **53** 499–516

Bueler E, Lingle C S, Kallen-Brown J A, Covey D N and Bowman L N 2005 Exact solutions and verification of numerical models for isothermal ice sheets *J. Glaciol.* **51** 291–306

Burton J C, Amundson J M, Abbot D S, Boghosian A, Cathles L M, Correa-Legisos S, Darnell K N, Guttenberg N, Holland D M and MacAyeal D R 2012 Laboratory investigations of iceberg capsize dynamics, energy dissipation and tsunamigenesis *J. Geophys. Res.* **117** F01007

Carr J R, Vieli A and Stokes C 2013 Influence of sea ice decline, atmospheric warming, and glacier width on marine-terminating outlet glacier behavior in northwest Greenland at seasonal to interannual timescales *J. Geophys. Res.: Earth Surf.* **118** 1210–26

Cazenave A and Remy F 2011 Sea-level and climate: measurements and causes of changes, WIREs *Clim. Change* **2** 647–62

Chen J L, Wilson C R and Tapley B D 2006 Satellite gravity measurements confirm accelerated melting of Greenland ice sheet *Science* **313** 1958–60

Cheng M and Tapley B D 2004 Variations in the Earth's oblateness during the past 28 years *J. Geophys. Res.* **109** B09402

Christensen O B, Drews M, Christensen J, Dethloff K, Ketelsen K, Hebestadt I and Rinke A 2006 *The HIRHAM Regional Climate Model* Version 5, *Technical Report* 06-17, *DMI technical report* Cambridge University Press, Cambridge available at (www.dmi.dk/dmi/tr06-17.pdf)

Christoffersen P, O'Leary M, Van Angelen J H and Van Den Broeke M 2012 Partitioning effects from ocean and atmosphere on the calving stability of Kangerdlugssuaq Glacier, East Greenland *Ann. Glaciol.* **53** 249–56

Church J A and White N J 2006 A 20th century acceleration in global sea-level rise *Geophys. Res. Lett.* **33** L01602

Csatho B, Schenk T, Van Der Veen C J and Krabill W B 2008 Intermittent thinning of Jakobshavn Isbræ, West Greenland, since the Little Ice Age *J. Glaciol.* **54** 131–44

Dahl-Jensen D, Gundestrup N S, Gogineni S and Miller H 2003 Basal melt at NorthGRIP modeled from borehole, ice-core and radio-echo sounder observations *Ann. Glaciol.* **37** 207–12

Das S B *et al* 2008 Fracture propagation to the base of the Greenland ice sheet during supraglacial lake drainage *Science* **320** 778–81

Davis C H and Ferguson A C 2004 Elevation change of the Antarctic ice sheet, 1995–2000, from ERS-2 satellite radar altimetry *IEEE Trans. Geosci. Remote* **42** 2437–45

de Fleurian B *et al* 2014 A double continuum hydrological model for glacier applications *The Cryosphere* **8** 137–53

Duval P 1977 The role of water content on the creep of polycrystalline ice *IAHS-AISH* **118** 29–33

Dziewonski A and Anderson D 1981 Preliminary reference Earth model *Phys. Earth Planet. Inter.* **25** 297–356

Edwards T L *et al* 2014a Probabilistic parameterisation of the surface mass balance-elevation feedback in regional climate model simulations of the Greenland ice sheet *Cryosphere* **8** 181–94

Edwards T L *et al* 2014b Effect of uncertainty in surface mass balance-elevation feedback on projections of the future sea level contribution of the Greenland ice sheet *Cryosphere* **8** 195–208

Enderlin E M and Howat I M 2013 Submarine melt rate estimates for floating termini of Greenland outlet glaciers (2000–2010) *J. Glaciol.* **59** 67–75

Enderlin E M, Howat I M, Jeong S, Noh M-J, van Angelen J H and van den Broeke M R 2014 An improved mass budget for the Greenland ice sheet *Geophys. Res. Lett.* **41** 866–72

Enderlin E M, Howat I M and Vieli A 2013 High sensitivity of tidewater outlet glacier dynamics to shape *Cryosphere* **7** 1007–15

Ettema J, van den Broeke M R, van Meijgaard E, van de Berg W J, Bamber J L, Box J E and Bales R C 2009 Higher surface mass balance of the Greenland ice sheet revealed by high-resolution climate modeling *Geophys. Res. Lett.* **36** L12501

Ewert H, Groh A and Dietrich R 2012 Volume and mass changes of the Greenland ice sheet inferred from ICESat and GRACE *J. Geodyn.* **59–60** 111–23

Fahnestock M, Abdalati W, Joughin I, Brozena J and Gogineni P 2001 High geothermal heat flow, Basal melt and the origin of rapid ice flow in central Greenland *Science* **294** 2338–42

Falkner K *et al* 2011 Context for the recent massive Petermann Glacier calving event, Eos *Trans. AGU* **92** 2010–2

Fettweis X, Tedesco M, van den Broeke M and Ettema J 2011 Melting trends over the Greenland ice sheet (1958–2009) from spaceborne microwave data and regional climate models *Cryosphere* **5** 359–75

Fischer R, Nowicki S, Kelley M and Schmidt G A 2014 A system of conservative regridding for ice atmosphere coupling in a General Circulation Model (GCM) *Geosci. Model Dev.* **7** 883–907

Fox Maule C, Purucker M E, Olsen N and Mosegaard K 2005 Heat flux anomalies in Antarctica revealed by satellite magnetic data *Science* **309** 464–7

Franco B, Fettweis X, Lang C and Erpicum M 2012 Impact of spatial resolution on the modelling of the Greenland ice sheet surface mass balance between 1990–2010, using the regional climate model MAR *Cryosphere* **6** 695–711

Fürst J J, Goelzer H and Huybrechts P 2013 Effect of higher-order stress gradients on the centennial mass evolution of the Greenland ice sheet *Cryosphere* **7** 183–99

Fyke J G, Vizcaíno M, Lipscomb W and Price S 2014 Future climate warming increases Greenland ice sheet surface mass balance variability *Geophys. Res. Lett.* **41** 470–5

Gagliardini O *et al* 2013 Capabilities and performance of Elmer/Ice, a new-generation ice sheet model *Geosci. Model Dev.* **6** 1299–318

Gillet-Chaulet F, Gagliardini O, Seddik H, Nodet M, Durand G, Ritz C, Zwinger T, Greve R and Vaughan D G 2012 Greenland ice sheet contribution to sea-level rise from a new-generation ice-sheet model *Cryosphere* **6** 1561–76

Greve R and Blatter H 2009 *Dynamics of Ice Sheets and Glaciers* (Dordrecht: Springer-Verlag) [ISBN 978-3-642-03414-5]

Groh A, Ewert H, Fritsche M, Rülke A, Rosenau R, Scheinert M and Dietrich R 2014 Assessing the current evolution of the Greenland ice sheet by means of satellite and ground-based observations *Surv. Geophys.* **35** 1459–80

Hanna E *et al* 2005 Runoff and mass balance of the Greenland Ice Sheet: 1958–2003 *J. Geophys. Res.* **110** D13108

Hanna E *et al* 2011 Greenland ice sheet surface mass balance 1870–2010 based on twentieth century reanalysis, and links with global climate forcing *J. Geophys. Res.* **116** D24121

Hanna E, Fettweis X, Mernild S H, Cappelen J, Ribergaard M H, Shuman C A, Steffen K, Wood L and Mote T L 2014 Atmospheric and oceanic climate forcing of the exceptional Greenland ice sheet surface melt in summer 2012 *Int. J. Climatol.* **34** 1022–37

Helm V, Humbert A and Miller H 2014 Elevation and elevation change of Greenland and Antarctica derived from CryoSat-2 *Cryosphere* **8** 1539–59

Helsen M M, van de Wal R S W, van den Broeke M R, van de Berg W J and Oerlemans J 2012 Coupling of climate models and ice sheet models by surface mass balance gradients: application to the Greenland ice sheet *Cryosphere* **6** 255–72

Hewitt I J 2011 Modelling distributed and channelized subglacial drainage: the spacing of channels *J. Glaciol.* **57** 302–14
Higgins A 1991 North Greenland glacier velocities and calf ice production *Polarforschung* **60** 1–23 (http://epic.awi.de/28269/1/Polarforsch1990_1_1.pdf)
Hofton M A, Blair J B, Luthcke S B and Rabine D L 2008 Assessing the performance of 20–25 m footprint waveform lidar data collected in ICESat data corridors in Greenland *Geophys. Res. Lett.* **35** L24501
Hofton M A, Luthcke S B and Blair J B 2013 Estimation of ICESat intercampaign elevation biases from comparison of lidar data in East Antarctica *Geophys. Res. Lett.* **40** 5698–703
Holland D, Thomas R, Young B, Ribergaard M H and Lyberth B 2008 Acceleration of Jakobshavn Isbræ triggered by warm subsurface ocean waters *Nat. Geosci.* **1** 659–64
Howat I M, Ahn Y, Joughin I, van den Broeke M R, Lenaerts J T M and Smith B 2011 Mass balance of Greenland's three largest outlet glaciers, 2000–2010 *Geophys. Res. Lett.* **38** L12501
Howat I and Eddy A 2011 Multi-decadal retreat of Greenland's marine-terminating glaciers *J. Glaciol.* **57** 389–96
Howat I M, Joughin I and Scambos T 2007 Rapid changes in ice discharge from Greenland outlet glaciers *Science* **315** 1559–61
Howat I M, Joughin I, Tulaczyk S and Gogineni S 2005 Rapid retreat and acceleration of Helheim Glacier, east Greenland *Geophys. Res. Lett.* **32** L22502
Howat I M, Smith B E, Joughin I and Scambos T A 2008 Rates of southeast Greenland ice volume loss from combined ICESat and ASTER observations *Geophys. Res. Lett.* **35** 1–5
Hurkmans R T W L, Bamber J L, Davis C H, Joughin I R, Khvorostovsky K S, Smith B S and Schoen N 2014 Time-evolving mass loss of the Greenland ice sheet from satellite altimetry *Cryosphere* **8** 1725–40
Hutter K 1983 *Theoretical Glaciology; Material Science of Ice and the Mechanics of Glaciers and Icesheets* (Dordrecht and Tokyo: Reidel/Terra Scientific)
Iken A 1978 Variations of surface velocities of some Alpine glaciers measured at intervals of a few hours. Comparison with Arctic glaciers *Zeitschrift fuer Gletscherkunde und Glazialgeologie* **13** 23–35
Iken A 1981 The effect of the subglacial water pressure on the sliding velocity of a glacier in an idealized numerical model. *J. Glaciol.* **27** 407–21
IPCC 2007 *Climate Change 2007, The Physical Science Basis. Contribution of Working Group I to the Fourth Assessment Report of the Intergovernmental Panel on Climate Change* (Cambridge: Cambridge University Press)
Jacob T, Wahr J, Pfeffer W T and Swenson S 2012 Recent contributions of glaciers and ice caps to sea-level rise *Nature* **482** 514–8
Jensen D 1977 A 3D polar ice-sheet model *J. Glaciol.* **18** 333–89
Johannessen O M, Khvorostovsky K, Miles M W and Bobylev L P 2005 Recent ice-sheet growth in the interior of Greenland *Science* **310** 1013–6
Joughin I 2002 Ice-sheet velocity mapping: a combined interferometric and speckle-tracking approach *Ann. Glaciol.* **34** 195–201
Joughin I, Howat I M, Fahnestock M, Smith B, Krabill W, Alley R B, Stern H and Truffer M 2008a Continued evolution of Jakobshavn Isbræ following its rapid speedup *J. Geophys. Res.* **113** F04006
Joughin I *et al* 2008b Seasonal speedup along the western flank of the Greenland ice sheet *Science* **320** 781
Joughin I, Abdalati W and Fahnestock M 2004 Large fluctuations in speed on Greenland's Jakobshavn Isbrae glacier *Nature* **432** 608–10
Joughin I, Smith B, Howat I M, Scambos T and Moon T 2010 Greenland flow variability from ice-sheet-wide velocity mapping *J. Glaciol.* **56** 415–30
Joughin I *et al* 2012 Seasonal to decadal scale variations in the surface velocity of Jakobshavn Isbrae, Greenland: Observation and model-based analysis *J. Geophys. Res.* **117** F02030
Joughin I, Smith B E and Medley B 2014a Marine ice sheet collapse potentially underway for the Thwaites Glacier Basin, West Antarctica *Science* **344** 735–8
Joughin I, Smith B E, Shean D E and Floricioiu D 2014b Brief communication: further summer speedup of Jakobshavn Isbræ *Cryosphere* **8** 209–14
Kelley S E, Briner J P, Young N E, Babonis G S and Csato B 2012 Maximum late Holocene extent of the western Greenland ice sheet during the late 20th century *Quat. Sci. Rev.* **56** 89–98
Khan S A *et al* 2014a Sustained mass loss of the northeast Greenland ice sheet triggered by regional warming *Nat. Clim. Change* **4** 292–9
Khan S A *et al* 2014b Glacier dynamics at Helheim and Kangerdlugssuaq glaciers, southeast Greenland, since the Little Ice Age *Cryosphere* **8** 1497–507
Khan S A *et al* 2013 Recurring dynamically induced thinning during 1985–2010 on Upernavik Isstrøm, West Greenland *J. Geophys. Res.-Earth Surf.* **118** 111–21
Khan S A, Wahr J, Bevis M, Velicogna I and Kendrick E 2010a Spread of ice mass loss into northwest Greenland observed by GRACE and GPS *Geophys. Res. Lett.* **37** L06501
Khan S A, Liu L, Wahr J, Howat I, Joughin I, van Dam T and Fleming K 2010b GPS measurements of crustal uplift near Jakobshavn Isbræ due to glacial ice mass loss *J. Geophys. Res.* **115** B09405
Khvorostovsky K S 2012 Merging and analysis of elevation time series over Greenland ice sheet from satellite radar altimetry *IEEE Trans. Geosci. Remote* **50** 23–36 1059–61
Kjeldsen K K *et al* 2013 Improved ice loss estimate of the northwestern Greenland ice sheet *J. Geophys. Res. Solid Earth* **118** 698–708
Kjær K H *et al* 2012 Aerial photographs reveal late-20th-century dynamic ice loss in northwestern Greenland *Science* **337** 569–73
Krabill W *et al* 1999 Rapid thinning of parts of the Southern Greenland ice sheet *Science* **283** 1522–4
Krabill W *et al* 2000 Greenland ice sheet: high-elevation balance and peripheral thinning *Science* **289** 428–30
Krabill W B *et al* 2002 Aircraft laser altimetry measurement of elevation changes of the Greenland ice sheet: technique and accuracy assessment *J. Geodyn.* **34** 357–76
Krabill W B *et al* 2004 Greenland ice sheet: increased coastal thinning *Geophys. Res. Lett.* **31** L24402
Kusche J, Schmidt R, Petrovic S and Rietbroek R 2009 Decorrelated GRACE time-variable gravity solutions by GFZ, and their validation using a hydrological model *J. Geod.* **83** 903–13
Landerer F W and Swenson S C 2012 Accuracy of scaled GRACE terrestrial water storage estimates *Water Resources Res.* **48** W04531
Larour E, Seroussi H, Morlighem M and Rignot E 2012a Continental scale, high order, high spatial resolution, ice sheet modeling using the ice sheet system model (ISSM) *J. Geophys. Res.***117** F01022
Larour E, Schiermeier J, Rignot E, Seroussi H, Morlighem M and Paden J 2012b Sensitivity analysis of Pine Island Glacier ice flow using ISSM and DAKOTA *J. Geophys. Res.* **117** F2009
Larour E *et al* 2014 Inferred basal friction and surface mass balance of the Northeast Greenland Ice Stream using data assimilation of ICESat (Ice Cloud and land Elevation Satellite) surface altimetry and ISSM (Ice Sheet System Model) *The Cryosphere* **8** 2335–51
Lea J M., Mair D W F, Nick F M, Rea B R, Weidick A, Kjær K H, Morlighem M, van As D and Schofield J E 2014

Terminus-driven retreat of a major southwest Greenland tidewater glacier during the early 19th century: insights from glacier reconstructions and numerical modelling *J. Glaciol.* **60**

Lecleqer P W, Oerlemans J, Basagic H J, Bushueva I, Cook A J and Le Bris R 2014 A data set of worldwide glacier length fluctuations *Cryosphere* **8** 659–72

Leng W, Ju L, Gunzburger M and Price S 2013 Manufactured solutions and the verification of 3D Stokes ice-sheet models *Cryosphere* **7** 19–29

Leverman A, Albrecht T, Winkelmann R, Martin M A, Haseloff M and Joughin I 2012 Kinematic first-order calving law implies potential for abrupt ice-shelf retreat *Cryosphere* **6** 273–86

Levermann A *et al* 2011 Potential climatic transitions with profound impact on Europe, review of the current state of six tipping elements of the climate system *Clim. Change* **110** 845–78

Liu L, Wahr J, Howat I, Khan S A, Joughin I and Furuya M 2012 Constraining ice mass loss from Jakobshavn Isbræ (Greenland) using InSAR-measured crustal uplift *Geophys. J. Int.* **188** 994–1006

Lliboutry L A and Duval P 1985 Various isotropic and anisotropic ices found in glaciers and polar ice caps and their corresponding rheologies *Annales Geophys.* **3** 207–24

Luckman A, Murray T, de Lange R and Hanna E 2006 Rapid and synchronous ice-dynamic changes in East Greenland *Geophys. Res. Lett*. **33** L03503

Luthke S B, Zwally H J, Abdalati W, Rowlands D D, Ray R D, Nerem R S, Lemoine F G, McCarthy J J and Chinn D S 2006 Recent Greenland ice mass loss by drainage system from satellite gravity observations *Science* **314** 1286–9

McFadden E M, Howat I M, Joughin I, Smith B E and Ahn Y 2011 Changes in the dynamics of marine terminating outlet glaciers in west Greenland (2000–2009) *J. Geophys. Res.* **116** F02022

Mercer J 1978 West Antarctic ice sheet and CO_2 greenhouse effect: a threat of disaster *Nature* **271** 321–5

Moon T and Joughin I 2008 Changes in ice front position on Greenland's outlet glaciers from 1992 to 2007 *J. Geophys. Res.* **113** F02022

Moon T, Joughin I, Smith B and Howat I 2012 21st-century evolution of Greenland outlet glacier velocities *Science* **336** 576–8

Morlighem M, Rignot E, Mouginot J, Seroussi H, and Larour E 2014 Deeply incised submarine glacial valleys beneath the Greenland ice sheet *Nat. Geosci.* **7** 418–22

Morlighem M, Rignot E, Mouginot J, Wu X, Seroussi H, Larour E and Paden J 2013 Highresolution bed topography mapping of Russell Glacier, Greenland, inferred from Operation IceBridge data *J. Glaciol.* **59** 1015–23

Motyka R J, Fahnestock M and Truffer M 2010 Volume change of Jakobshavn Isbræ, West Greenland?: 1985–1997–2007 *J. Glaciol*. **56** 635–46

Motyka R J, Truffer M, Fahnestock M, Mortensen J, Rysgaard S and Howat I 2011 Submarine melting of the 1985 Jakobshavn Isbræ floating tongue and the triggering of the current retreat *J. Geophys. Res*. **116** F01007

Murray T *et al* 2010 Ocean regulation hypothesis for glacier dynamics in southeast Greenland and implications for ice sheet mass changes *J. Geophys. Res.* **115** F03026

Näslund J-O, Jansson P, Fastook J L, Johnson J and Andersson L 2005 Detailed spatially distributed geothermal heat-flow data for modeling of basal temperatures and meltwater production beneath the Fennoscandian ice sheet *Annals of Glaciology* **40** 95–101

Nick F M *et al* 2012 The response of Petermann Glacier, Greenland, to large calving events, and its future stability in the context of atmospheric and oceanic warming *J. Glaciol*. **58** 229–39

Nick F M, Vieli A, Andersen M L, Joughin I, Payne A, Edwards T L, Pattyn F and van de Wal R S W 2013 Future sea-level rise from Greenland's main outlet glaciers in a warming climate *Nature* **497** 235–8

Nick F M, Vieli A, Howat I M and Joughin I 2009 Large-scale changes in Greenland outlet glacier dynamics triggered at the terminus *Nat. Geosci.* **2** 110–4

Nielsen M 2011 *Reinventing Discovery: The New Era of Networked Science* (Princeton, NJ: Princeton University Press)

Nowicki S *et al* 2013 Insights into spatial sensitivities of ice mass response to environmental change from the SeaRISE ice sheet modeling project II: Greenland *J. Geophys. Res*. **118** 1025–44

Palmer S, Shepherd A, Nienow P and Joughin I 2011 Seasonal speedup of the Greenland ice sheet linked to routing of surface water *Earth Planet. Sci. Lett.* **302** 423–8

Pattyn F *et al* 2012 Results of the marine ice sheet model Intercomparison project, MISMIP *Cryosphere* **6** 573–88

Peltier W R 2004 Global glacial isostasy and the surface of the ice-age Earth: The ICE-5G (VM2) model and GRACE *Annu. Rev. Earth Planet. Sci*. **32**, 111–49

Petrov L and Boy J-P 2004 Study of the atmospheric pressure loading signal in VLBI observations *J. Geophys. Res*. **109** B03405

Pfeffer W T 2007 A simple mechanism for irreversible tidewater glacier retreat *J. Geophys. Res.* **112** F03S25

Podlech S, Mayer C and Boggild C E 2004 Glacier retreat, mass-balance and thinning: Sermilik Glacier, South Greenland *Geogr. Ann. Ser. A Phys. Geogr*. **86** 305–17

Pralong A and Funk M 2005 Dynamic damage model of crevasse opening and application to glacier calving *J. Geophys. Res*. **110** 1–12

Price S F, Payne A J, Howat I M and Smith B E 2011 Committed sea-level rise for the next century from Greenland ice sheet dynamics during the past decade *Proc. Natl Acad. Sci. USA* **108** 8978–83

Pritchard H D, Arthern R J, Vaughan D G and Edwards L 2009 Extensive dynamic thinning on the margins of the Greenland and Antarctic ice sheets *Nature* **461** 971–5

Ramillien G, Lombard A, Cazenave A, Ivins E R, Llubes M, Remy F and Biancale R 2006 Interannual variations of the mass balance of the Antarctica and Greenland ice sheets from GRACE *Glob. Planet. Change* **53** 198–208

Reeh N 2008 A nonsteady-state firn-densication model for the percolation zone of a glacier *J. Geophys. Res*. **113** F03023

Reeh N, Thomsen H H, Higgins A K and Weidick A 2001 Sea ice and the stability of north and northeast Greenland floating glaciers *Ann. Glaciol*. **33** 474–80

Remy F and Parouty S 2009 Antarctic ice sheet and radar altimetry: a review *Remote Sens*. **1** 1212–39

Rignot E, Box J E, Burgess E and Hanna E 2008 Mass balance of the Greenland ice sheet from 1958 to 2007 *Geophys. Res. Lett*. **35** L20502

Rignot E, Gogineni S, Joughin I and Krabill W B 2001 Contribution to the glaciology of northern Greenland from satellite radar interferometry *J. Geophys. Res.* **106** 7–19

Rignot E and Kanagaratnam P 2006 Changes in the velocity structure of the Greenland ice sheet *Science* **311** 986–90

Rignot E, Koppes M and Velicogna I 2010 Rapid submarine melting of the calving faces of West Greenland glaciers *Nature Geosci.* **3** 187–91

Rignot E, Velicogna I, van den Broeke M R, Monaghan A and Lenaerts J 2011 Acceleration of the contribution of the Greenland and Antarctic ice sheets to sea level rise *Geophys. Res. Lett.* **38** L05503

Roache P J 1998 *Verification and Validation in Computational Science and Engineering* (Albuquerque, New Mexico: Hermosa Publishers)

Robison R A V, Huppert H E and GraeWorster M 2010 Dynamics of viscous grounding lines *J. Fluid Mech*. **648** 363–80
Sasgen I, van den Broeke M, Bamber J L, Rignot E, Sørensen L S, Wouters B, Martinec Z, Velicogna I and Simonsen S B 2012 Timing and origin of recent regional ice-mass loss in Greenland *Earth Planet. Sci. Lett*. **333–334** 293–303
Schenk T, Csatho B, van der Veen C and McCormick D 2014 Fusion of multi-sensor surface elevation data for improved characterization of rapidly changing outlet glaciers in Greenland *Remote Sens. Environ.* **149** 239–51
Schild K M and Hamilton G S 2013 Seasonal variations of outlet glacier terminus position in Greenland *J. Glaciol*. **59** 759–70
Schoof C 2007 Ice sheet grounding line dynamics: steady states, stability, and hysteresis *J. Geophys. Res.* **112** F03S28
Schoof C 2010 Ice-sheet acceleration driven by melt supply variability *Nature* **468** 803–6
Screen J, Simmonds I and Keay K 2011 Dramatic inter-annual changes of perennial Arctic sea ice linked to abnormal summer storm activity *J. Geophys. Res*. **116** D15105
Seale A, Christoffersen P, Mugford R I and O'Leary M 2011 Ocean forcing of the Greenland ice sheet: calving fronts and patterns of retreat identified by automatic satellite monitoring of eastern outlet glaciers *J. Geophys. Res*. **116** F03013
Seddik H, Greve R, Zwinger T, Gillet-Chaulet F and Gagliardini O2012 Simulations of the Greenland ice sheet 100 years into the future with the full Stokes model Elmer/Ice *J. Glaciol.* **58** 427–40
Seroussi H, Dhia H B, Morlighem M, Larour E, Rignot E and Aubry D 2012 Coupling ice flow models of varying orders of complexity with the Tiling method *J. Glaciol*. **58** 776–86
Seroussi H, Morlighem M, Rignot E, Larour E, Aubry D, Ben Dhia H and Kristensen S S 2011 Ice flux divergence anomalies on 79north Glacier, Greenland *Geophys. Res. Lett*. **38** 1–5
Seroussi H *et al* 2013 Dependence of century-scale projections of the Greenland ice sheet on its thermal regime *J. Glaciol.* **59** 1024–34
Shapiro N M and Ritzwoller M H 2004 Inferring surface heat flux distributions guided by a global seismic model: particular application to Antarctica *Earth Planet. Sc. Lett.* **223** 213–24
Shepherd A *et al* 2012 A reconciled estimate of ice-sheet mass balance *Science* **338** 1183–9
Shepherd A, Hubbard A L, Nienow P, King M, McMillan M and Joughin I 2009 Greenland ice sheet motion coupled with daily melting in late summer *Geophys. Res. Lett.* **36** L01501
Siegfried M R, Hawley R L and Burkhart J F 2011 High-resolution ground-based GPS measurements show intercampaign bias in ICESat elevation data near Summit, Greenland *IEEE Trans. Geosci. Remote* **49** 3393–400
Siemes C, Ditmar P, Riva R E M, Slobbe D C, Liu X L and Farahani H H2013 Estimation of mass change trends in the Earth's system on the basis of GRACE satellite data, with application to Greenland *J Geod*. **87** 69–87
Simpson M J R, Wake L, Milne G A and Huybrechts P 2011 The influence of decadal- to millennial-scale ice mass changes on present-day vertical land motion in Greenland: implications for the interpretation of GPS observations *J. Geophys. Res*. **116** B02406
Slobbe D C, Ditmar P and Lindenbergh R C 2009 Estimating the rates of mass change, ice volume change and snow volume change in Greenland from ICESat and GRACE data *Geophys. J. Int.* **176** 95–106
Sørensen L S, Simonsen S B, Nielsen K, Lucas-Picher P, Spada G, Adalgeirs-dottir G, Forsberg R and Hvidberg C S 2011 Mass balance of the Greenland ice sheet (2003–2008) from ICESat data—the impact of interpolation, sampling and firn density *Cryosphere* **5** 173–86
Stearns L A and Hamilton G S 2007 Rapid volume loss from two East Greenland outlet glaciers quantified using repeat stereo satellite imagery *Geophys. Res. Lett*. **34** L05503
Straneo F, Hamilton G S, Sutherland D A, Stearns L A, Davidson F, Hammill M O, Stenson G B and Rosing-Asvid A 2010 Rapid circulation of warm subtropical waters in a major glacial fjord in East Greenland *Nat. Geosci*. **3** 182–6
Straneo F and Heimbach P 2013 North Atlantic warming and the retreat of Greenland's outlet glaciers *Nature* **504** 36–43
Straneo F, Sutherland D A, Holland D, Gladish C, Hamilton G S, Johnson H L, Rignot E, Xu Y and Koppes M 2012 Characteristics of ocean waters reaching Greenland's glaciers *Ann. Glaciol*. **53** 202–10
Stroeve J C, Serreze M C, Holland M M, Kay J, Maslanik J and Barrett A P 2012 The Arctic's rapidly shrinking sea ice cover: a research synthesis *Clim. Change* **110** 1005–27
Sundal A, Shepherd A, Nienow P, Hanna E, Palmer S and Huybrechts P 2011 Melt-induced speed-up of Greenland ice sheet offset by efficient subglacial drainage *Nature* **469** 521–4
Sutterley T C, Velicogna I, Csatho B, van den Broeke M, Rezvan-Behbahani S and Babonis G 2014 Evaluating Greenland glacial isostatic adjustment corrections using GRACE, altimetry and surface mass balance data *Environ. Res. Lett*. **9**
Swenson S, Chambers D and Wahr J 2008 Estimating geocenter variations from a combination of GRACE and ocean model output *J. Geophys. Res*. **113** B08410
Tapley B D, Bettadpur S, Watkins M and Reigber C 2004 The gravity recovery and climate experiment: mission overview and early results *Geophys. Res. Lett*. **31** L09607
Tedesco M, Fettweis X, Mote T, Wahr J, Alexander P, Box J E and Wouters B 2013 Evidence and analysis of 2012 Greenland records from spaceborne observations, a regional climate model and reanalysis data *Cryosphere* **7** 615–30
Tedesco M, Fettweis X, van den Broeke M R, van de Wal R S W, Smeets C J P P, van de Berg W J, Serreze M C and Box J E 2011 The role of albedo and accumulation in the 2010 melting record in Greenland *Environ. Res. Lett*. **6** 014005
Thomas R H 1979 The dynamics of marine ice sheets *J. Glaciol.* **24** 167–77
Thomas R H, Frederick E, Krabill W, Manizade S and Martin C 2006 Progressive increase in ice loss from Greenland *Geophys. Res. Lett.* **33** L10503
Van As D *et al* 2014 Increasing meltwater discharge from the Nuuk region of the Greenland ice sheet and implications for mass balance (1960–2012) *J. Glaciol*. **60** 314–22
van den Broeke M, Bamber J, Ettema J, Rignot E, Schrama E, van de Berg W J, van Meijgaard E, Velicogna I and Wouters B 2009 Partitioning recent Greenland mass loss *Science* **326** 984–6
van de Wal R S W and Oerlemans J 1994 An energy balance model for the Greenland ice sheet *Glob. Planet. Change* **9** 115–31
Vaughan D G and Arthern R 2007 Why is it hard to predict the future of ice sheets? *Science* **315** 1503–4
Vaughan D G *et al* 2013 Observations: Cryosphere *Climate Change 2013: the Physical Science Basis. Contribution of Working Group I to the Fifth Assessment Report of the Intergovernmental Panel on Climate Change* ed T F Stocker *et al* (Cambridge: Cambridge University Press)
Velicogna I 2009 Increasing rates of ice mass loss from the Greenland and Antarctic ice sheets revealed by GRACE *Geophys. Res. Lett*. **36** L19503
Velicogna I, Sutterley T C and van den Broeke M R 2014 Regional acceleration in ice mass loss from Greenland and Antarctica using GRACE time-variable gravity data *Geophys. Res. Lett*. **41** 8130–7

Velicogna I and Wahr J 2006 Acceleration of Greenland ice mass loss in spring 2004 *Nature* **443** 328–31
Velicogna I and Wahr J 2013 Time-variable gravity observations of ice sheet mass balance: precision and limitations of the GRACE satellite data *Geophys. Res. Lett.* **40** 3055–63
Vizcaíno M 2014 Ice sheets as interactive components of earth system models: progress and challenges *WIREs Clim. Change* **5** 557–68
Vizcaíno M, Lipscomb W H, Sacks W J, van Angelen J H, Wouters B and van den Broeke M R 2013 Greenland surface mass balance as simulated by the community earth system model. Part I: model evaluation and 1850–2005 results *J. Clim.* **26** 7793–812
Vizcaíno M, Lipscomb W H, Sacks W J and van den Broeke M 2014 Greenland surface mass balance as simulated by the community earth system model. Part II: twenty-first-century changes *J. Clim.* **27** 215–26
Wahr J, Molenaar M and Bryan F 1998 Time-variability of earth's gravity field: hydrological and oceanic effects and their possible detection using GRACE *J. Geophys. Res.* **113** 30.205–29
Wake L M, Huybrechts P, Box J E, Hanna E, Janssens I and Milne G A 2009 Surface mass-balance changes of the Greenland ice sheet since 1866 *Ann. Glaciol.* **50** 178–84
Walsh K, Howat I, Ahn Y and Enderlin E 2012 Changes in the marine-terminating glaciers of central east Greenland, 2000–2010 *Cryosphere* **6** 211–20
Wang J, Zhang J, Watanabe E, Ikeda M, Mizobata K, Walsh J E, Bai X and Wu B 2009 Is the dipole anomaly a major driver to record lows in Arctic summer sea ice extent? *Geophys. Res. Lett.* **36** L05706
Warren C R and Glasser N F 1992 Contrasting response of South Greenland Glaciers to recent climatic change *Arct. Antarct. Alp. Res.* **24** 124–32
Werder M A, Hewitt I J, Schoof C G and Flowers G E 2013 Modeling channelized and distributed subglacial drainage in two dimensions *J. Geophys. Res* **118** 2140–58
Weertman J 1974 Stability of the junction of an ice sheet and an ice shelf *J. Glaciol.* **13** 3–11
Weidick A 1959 Glacial variations in West Greenland in historical time *Meddelser om Grønland* **158** 1–196
Weidick A 1968 Observations on some Holocene glacier fluctuations in West Greenland *Meddelser om Grønland* **165** 1–202
Weidick A 1994 Historical fluctuations of calving glaciers in South and West Greenland *Geol. Greenland Surv. Bull.* **161** 73–9
Wingham D J, Ridout A L, Scharroo R, Arthern R J and Shum C K 1998 Antarctic elevation change from 1992 to 1996 *Science* **282** 456–8
Wouters B, Chanbers D and Schrama E J O 2008 GRACE observes small-scale mass loss in Greenland *Geophys. Res. Lett.* **35** L20501
Wouters B, Bamber J L, van den Broeke M R, Lenaerts J T M and Sasgen I 2013 Limits in detecting acceleration of ice sheet mass loss due to climate variability *Nat. Geosci.* **6** 613–6
Yang L 2011 A Southern Greenland ice sheet glacier discharge reconstruction: 1958–2007 *Phys. Procedia* **22** 292–8
Zuo Z and Oerlemans J 1997 Contribution of glacier melt to sea-level rise since AD 1865, a regionally differentiated calculation *Clim. Dyn.* **13** 832–45
Zwally H J, Abdalati W, Herring T, Larson K M, Saba J and Steffen K 2002 Surface melt-induced acceleration of Greenland ice-sheet flow *Science* **297** 218–22
Zwally H J, Giovinetto M B, Li J, Cornejo H G, Beckley M A, Brenner A C, Saba J L and Yi D 2005 Mass changes of the Greenland and Antarctic ice sheets and shelves and contributions to sea-level rise: 1992–2002 *J. Glaciol.* **51** 509–27
Zwally H J *et al* 2011 Greenland ice sheet mass balance: distribution of increased mass loss with climate warming; 2003–07 versus 1992–2002 *J. Glaciol.* **57** 88–102
Zwally H, Schutz R, Bentley C, Bufton J, Herring T, Minster J, Spinhirne J and Thomas R 2014 GLAS/ICESat L2 Antarctic and Greenland ice sheet altimetry data. Version 34 Boulder, Colorado USA, National Snow and Ice Data Center doi:10.5067/ICESAT/GLAS/DATA225